J. Fluid Mech. (1986), *vol.* 169, *pp.* 429–464
Printed in Great Britain

Resonant flow of a stratified fluid over topography

By R. H. J. GRIMSHAW† AND N. SMYTH†
Department of Mathematics, University of Melbourne, Parkville, Victoria 3052, Australia

(Received 24 July 1985 and in revised form 16 February 1986)

The flow of a stratified fluid over topography is considered in the long-wavelength weakly nonlinear limit for the case when the flow is near resonance; that is, the basic flow speed is close to a linear long-wave phase speed for one of the long-wave modes. It is shown that the amplitude of this mode is governed by a forced Korteweg–de Vries equation. This equation is discussed both analytically and numerically for a variety of different cases, covering subcritical and supercritical flow, resonant or non-resonant, and for localized forcing that has either the same, or opposite, polarity to the solitary waves that would exist in the absence of forcing. In many cases a significant upstream disturbance is generated which consists of a train of solitary waves. The usefulness of internal hydraulic theory in interpreting the results is also demonstrated.

1. Introduction

The flow of a stratified fluid over localized topography has been the subject of many theoretical and experimental studies. Most theoretical studies have been confined either to linearized theory, or to steady flow, for the two-dimensional flow of an inviscid incompressible fluid. Even so, these theories have provided useful models for such atmospheric phenomena as the generation of lee waves behind a mountain range, or for such oceanic phenomena as tidal flows over sills. Useful summaries and critiques of these classical theories have been given by McIntyre (1972) and Baines (1977). Most of the earlier studies were concerned with a description of the downstream stationary lee-wave field, and in this respect have been moderately successful. However, one of the more controversial issues has been the question of upstream influence; that is, to what extent do disturbances, generated in the vicinity of the topography by transient and nonlinear processes, propagate upstream and ultimately alter the initial upstream state of the fluid. McIntyre (1972), in extending earlier simpler theories of Benjamin (1970) and Keady (1971), performed an expansion with the ratio of the height of the topography to the total fluid depth as the small parameter and showed that the only significant upstream disturbances were weak second-order long-wave motions generated by nonlinear interactions in the lee-wave tails. However, Baines (1977, 1979), in a series of experiments with the flow of a continuously stratified fluid over an obstacle, found upstream disturbances that were first-order in the obstacle height, propagated with a long-wave speed and were generated by nonlinear processes over the obstacle. With particular pertinence to the theory developed in this paper, Baines observed that these upstream disturbances were very strong when the flow was near a resonance. Here a resonance is defined to mean a coincidence between the basic flow speed and one of the free long-wave speeds, with the consequence that in linearized theory the

† Current address: School of Mathematics, University of N.S.W., P.O. Box 1, Kensington, N.S.W. 2033, Australia.

corresponding long wave cannot propagate away from the obstacle. In hydraulic terminology the flow is said to be critical. In some later experiments with a two-layer fluid, Baines (1984) confirmed these findings and, in particular, showed that near resonance the main features of interest are nonlinear in character. Furthermore, Baines demonstrated the utility of internal hydraulic theory in describing his experimental results, and it should be noted that the upstream disturbances often had the character of undular bores.

Motivated by these results, we propose in this paper to present a theoretical study of the flow of a stratified fluid over localized topography for the case when the flow is near resonance. Since we anticipate that nonlinear long waves will form an essential feature of the description of resonant, or near-resonant, flow, we assume from the outset that the topography, although localized, has a long lengthscale relative to the total fluid depth, and construct our theory accordingly. In §2 we present the equations of motion for the two-dimensional flow of an inviscid incompressible fluid over localized topography, and construct the non-resonant theory. This reduces at leading order to linear long-wave theory. Then in §3 we consider the resonant case and show that the flow can be described by a forced Korteweg–de Vries (KdV) equation. Similar equations have recently been derived by Patoine & Warn (1982) and Malanotte-Rizzoli (1984) to describe the resonant forcing of Rossby waves by topography, and by Akylas (1984), Cole (1985) and Lee (1985) to describe the resonant forcing of water waves by a moving pressure distribution or bottom topography. With hindsight, it is not surprising that a forced KdV equation is the outcome of our analysis for the resonant case. Near resonance, a single mode dominates, and it is well known that free nonlinear long waves for this mode will be described by a free KdV equation (see e.g. the review by Grimshaw 1983). The presence of topographic forcing in effect supplies a forcing term to this equation.

In §4 we present some preliminary discussion and analysis of the forced KdV equation, which in scaled, non-dimensional form is given by (4.2a). Not surprisingly, in view of the results of Baines (1984), we find the hydraulic approximation, in which the dispersive term in the forced KdV equation is omitted, to be of great utility in our analysis provided that dispersion is invoked in the appropriate places to resolve shocks. Then in §§5 and 6 we present some numerical solutions of the forced KdV equation which, in total, give a comprehensive description of both the resonant and non-resonant cases for both positive and negative forcing. In §7 we summarize our results. Finally, in the Appendix we show briefly how the theory should be modified for the case when the total fluid depth is comparable to the horizontal lengthscale of the topography, but the stratification is effectively confined to a layer of small vertical extent.

2. Formulation

We shall consider the two-dimensional flow of an inviscid incompressible fluid. The coordinate system is sketched in figure 1. Throughout we shall use non-dimensional variables based on a lengthscale h_1, which is a typical vertical dimension of the waveguide, a timescale N_1^{-1}, where N_1 is a typical value of the Brunt–Väisälä frequency, and a pressure scale $\rho_1 g h_1$, where ρ_1 is a typical value of the density. These scales define the parameter $\beta = h_1 N_1^2 g^{-1}$, which is small in the Boussinesq approximation. We shall assume that the basic state has a constant horizontal velocity of magnitude V from left to right, a density $\rho_0(z)$ and a pressure $p_0(z)$, where $p_{0z} = -\rho_0$. The Brunt–Väisälä frequency $N(z)$ is defined by

$$\beta \rho_0 N^2 = -\rho_{0z}. \tag{2.1}$$

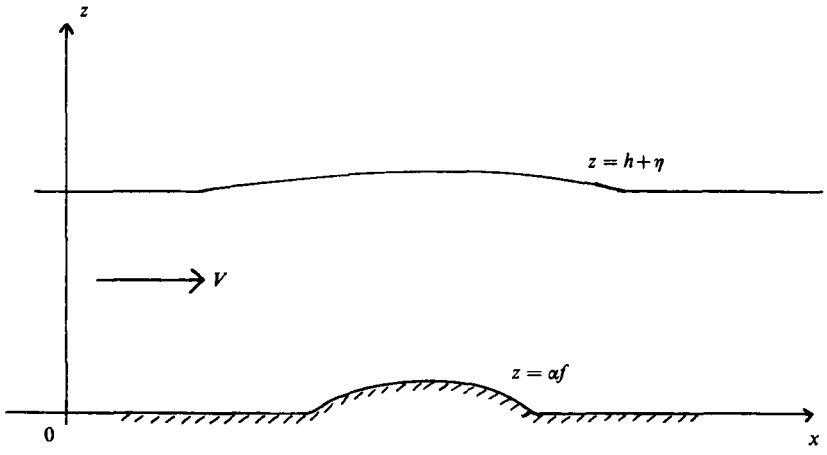

FIGURE 1. The coordinate system.

We shall find it convenient to introduce the vertical particle displacement ζ, so that the density is given by $\rho_0(z-\zeta)$. Then the equations of motion are

$$u_x + w_z = 0, \tag{2.2a}$$

$$\rho_0(z-\zeta)\frac{\mathrm{d}u}{\mathrm{d}t} + q_x = 0, \tag{2.2b}$$

$$\rho_0(z-\zeta)\frac{\mathrm{d}w}{\mathrm{d}t} + q_z + \frac{1}{\beta}\{\rho_0(z-\zeta) - \rho_0(z)\} = 0, \tag{2.2c}$$

$$w_0 = \frac{\mathrm{d}\zeta}{\mathrm{d}t}, \tag{2.2d}$$

where

$$\frac{\mathrm{d}}{\mathrm{d}t} = \frac{\partial}{\partial t} + (V+u)\frac{\partial}{\partial x} + w\frac{\partial}{\partial z}. \tag{2.2e}$$

Here u, w are the velocity components relative to the basic flow, and βq is the pressure relative to the basic state.

The bottom topography is given by

$$z = \alpha f(X, T), \tag{2.3a}$$

where

$$X = \epsilon x, \quad T = \epsilon t. \tag{2.3b}$$

Here α is a small parameter measuring the amplitude of the topography, and ϵ is a second small parameter such that ϵ^{-1} measures the horizontal lengthscale of the topography, which by hypothesis is to be much greater than the vertical dimension of the waveguide. Hence f depends on the slow space variable X. We shall also suppose that the topography is introduced slowly so that f also depends on the slow time variable T, and $f(X, 0) = 0$. At large times the topography attains its steady value $g(X)$, and hence we assume that

$$f(X, T) \sim g(X) \quad \text{as } T \to \infty. \tag{2.4}$$

We shall also assume that at all times the topography is localized, and $f(X, T) \to 0$ as $|X| \to \infty$. The bottom boundary condition is then

$$\zeta = \alpha f \quad \text{at } z = \alpha f. \tag{2.5}$$

We shall assume that the upper boundary is free and located at $z = h+\eta$, where h is a constant and η is the free-surface displacement. The top boundary conditions are then

$$\zeta = \eta \quad \text{at } z = h+\eta, \tag{2.6a}$$

$$p_0(h+\eta)+\beta q = p_0(h) \quad \text{at } z = h+\eta. \tag{2.6b}$$

If the upper boundary is rigid (2.6a, b) are replaced by $\zeta = 0$ on $z = h$. The modifications necessary in the subsequent analysis to deal with this case are left to the reader. To complete the problem specification we shall assume that the perturbation variables ζ, q and u are all zero at $t = 0$.

Since the forcing function f is $O(\alpha)$, we shall initially suppose that the response is also $O(\alpha)$. It will be shown later that this is valid only in the non-resonant cases, and at resonance a different scaling is required. We put

$$\left.\begin{aligned} \zeta &= \alpha\zeta_0(X, T; z)+\alpha^2\zeta_1+\ldots, \\ q &= \alpha q_0(X, T; z)+\alpha^2 q_1+\ldots, \\ u &= \alpha u_0(X, T; z)+\alpha^2 u_1+\ldots. \end{aligned}\right\} \tag{2.7}$$

Substitution into (2.2a–e), (2.5) and (2.6a, b), and neglect of terms that are relatively $O(\alpha)$ or $O(\epsilon^2)$, leads to the equations

$$u_{0X}+w_{0z} = 0, \tag{2.8a}$$

$$\rho_0(z)\frac{\mathrm{D}u_0}{\mathrm{D}T}+q_{0X} = 0, \tag{2.8b}$$

$$q_{0z}+\rho_0 N^2\zeta_0 = 0, \tag{2.8c}$$

$$w_0 = \frac{\mathrm{D}\zeta_0}{\mathrm{D}T}, \tag{2.8d}$$

where

$$\frac{\mathrm{D}}{\mathrm{D}T} = \frac{\partial}{\partial T}+V\frac{\partial}{\partial X}. \tag{2.8e}$$

The boundary conditions are

$$\zeta_0 = f \quad \text{at } z = 0, \tag{2.9a}$$

$$\rho_0\zeta_0 = \beta q_0 \quad \text{at } z = h. \tag{2.9b}$$

In order to solve (2.8a–e) and (2.9a, b) we introduce the normal modes $\phi_s(z)$, $s = 0, 1, 2, \ldots$. They are defined by the eigenvalue problem

$$(\rho_0\phi_{sz})_z+\frac{\rho_0 N^2}{c_s^2}\phi_s = 0, \tag{2.10a}$$

$$\phi_s = 0 \quad \text{at } z = 0, \tag{2.10b}$$

$$\phi_s = \beta c_s^2\phi_{sz} \quad \text{at } z = h. \tag{2.10c}$$

Here c_s^{-2} is the eigenvalue, where c_s is the long-wave phase speed relative to a basic state at rest. The modes satisfy the orthogonality condition

$$c_s^2\int_0^h \rho_0\phi_{sz}\phi_{rz}\,\mathrm{d}z = \delta_{sr}I_s. \tag{2.11}$$

The modes form a complete set, and hence we put

$$\zeta_0 = \sum_0^\infty A_s(X,T)\,\phi_s(z), \tag{2.12a}$$

$$q_0 = \rho_0 \sum_0^\infty c_s^2 B_s(X,T)\,\phi_{sz}(z), \tag{2.12b}$$

$$u_0 = -\sum_0^\infty E_s(X,T)\,\phi_{sz}(z). \tag{2.12c}$$

From the orthogonality condition we deduce that

$$I_s A_s = c_s^2 \int_0^h \rho_0 \zeta_{0z} \phi_{sz}\,\mathrm{d}z, \tag{2.13}$$

with similar expressions for B_s and E_s. Substitution into (2.8*a–e*) and (2.9*a*, *b*) then shows that

$$B_s = A_s + F_s, \tag{2.14a}$$

$$E_{sX} = \frac{\mathrm{D}A_s}{\mathrm{D}T}, \tag{2.14b}$$

$$\frac{1}{c_s^2}\frac{\mathrm{D}^2}{\mathrm{D}T^2}A_s = \frac{\partial^2 A_s}{\partial X^2} + \frac{\partial^2 F_s}{\partial X^2}, \tag{2.14c}$$

where

$$I_s F_s = \rho_0 c_s^2 \phi_{sz}(0) f(X,T). \tag{2.14d}$$

Here, since f vanishes at $T = 0$, $F_s(X,0) = 0$, and from (2.4)

$$F_s(X,T) \sim G_s(X) \quad \text{as } T \to \infty, \tag{2.15a}$$

where

$$I_s G_s = \rho_0 c_s^2 \phi_{sz}(0)\, g(X). \tag{2.15b}$$

The initial conditions for (2.14*a–c*) are that A_s, B_s and E_s all vanish at $T = 0$.

Equation (2.14*c*) is the inhomogeneous one-dimensional wave equation whose solution can be obtained by standard methods. We find that

$$A_s = -\frac{\partial}{\partial X}\left[\frac{c_s}{2}\int_0^T \mathrm{d}T' \{F_s(X - c_s^+(T-T'), T') - F_s(X + c_s^-(T-T'), T')\}\right], \tag{2.16a}$$

where

$$c_s^\pm = c_s \pm V. \tag{2.16b}$$

We are concerned here with the solution as $T \to \infty$. Using (2.15*a*), and assuming the non-resonant case, $c_s \neq V$, we find that

$$A_s \sim -\frac{c_s^2}{c_s^2 - V^2} G_s(X) + \frac{c_s}{2c_s^+} G_s(X - c_s^+ T) + \frac{c_s}{2c_s^-} G_s(X + c_s^- T) \quad \text{as } T \to \infty. \tag{2.17}$$

If the topography is switched on at $T = 0$ so that $F_s = G_s(X)$ for $0 < T < \infty$, then (2.17) is the exact solution of (2.14*c*). The solution (2.17) consists of a stationary response proportional to $G_s(X)$, together with freely propagating long waves. Those waves with speed c_s^+ propagate downstream, while those waves with speed c_s^- propagate downstream if $c_s < V$, but propagate upstream if $c_s > V$. The former case corresponds to supercritical flow, and the latter case to subcritical flow (with respect to the sth mode). On a long timescale, $T \sim \alpha^{-1}$, the freely propagating waves will be affected by nonlinearity and dispersion, and will evolve, either into a finite number of solitary waves, or into an oscillatory wavetrain, both being solutions of

a free KdV equation. We shall not develop this analysis here, as this process occurs at large distances from the topography, where $|X| \sim \alpha^{-1}$. The appropriate KdV equation has been derived by many authors (see e.g. Grimshaw 1983), and the analysis describing the transition from a free linear long wave to a solution of the KdV equation will parallel the corresponding discussion for surface gravity waves given by Hammack & Segur (1978) and Miles (1978).

However, for the resonant case, $c_s = V$ ($c_s^- = 0$), when the flow is critical with respect to the sth mode, we find that

$$A_s \sim \frac{c_s T}{2} G_{sX}(X) - \frac{c_s}{2c_s^+}\{G_s(X) - G_s(X - c_s^+ T)\} \quad \text{as } T \to \infty. \tag{2.18}$$

The first term in this expression shows that A_s grows linearly with time as $T \to \infty$. Hence the expansion (2.7) is secular for large times, and a different scaling is required. This is the main subject of this paper and is taken up in §3. In particular, it will be shown that (2.18) is valid only for times $T \ll \alpha^{-\frac{1}{2}}$.

3. The resonant case; $c_n \approx V$

We shall now suppose that the nth mode is resonant, and $c_n \approx V$. At resonance, we anticipate that the forcing of amplitude α will achieve a balance, *inter alia*, with the leading-order quadratic nonlinear terms. Hence we expect the response to scale with $\alpha^{\frac{1}{2}}$. We shall also require a balance between nonlinearity and dispersion, and for a KdV system this requires $\epsilon^2 = \alpha^{\frac{1}{2}}$. Hence we put

$$\left.\begin{aligned} \zeta &= \alpha^{\frac{1}{2}} A(X,\tau)\,\phi_n(z) + \alpha\zeta_1 + \ldots, \\ q &= \alpha^{\frac{1}{2}}\rho_0 c_n^2\, A(X,\tau)\,\phi_{nz}(z) + \alpha q_1 + \ldots, \\ u &= -\alpha^{\frac{1}{2}} c_n\, A(X,\tau)\,\phi_{nz}(z) + \alpha u_1 + \ldots, \end{aligned}\right\} \tag{3.1a}$$

where

$$\tau = \alpha^{\frac{1}{2}} T \tag{3.1b}$$

$$V = c_n + \alpha^{\frac{1}{2}}\Delta. \tag{3.1c}$$

Here Δ is a detuning parameter, and we recall that X and T are defined by (2.3b). τ is a long time variable, and (3.1a) is a far-field or outer expansion which is required to match with the inner expansion (2.7), whose leading-order terms are described by (2.12a–c), (2.17) and (2.18).

The leading order terms in (3.1a) satisfy (2.8a–d), the boundary condition (2.9b) and the homogeneous form of the boundary condition (2.9a) (i.e. replace f by zero). On substituting (3.1a) into (2.2a–d), (2.5) and (2.6a, b), we obtain

$$u_{1X} + \frac{\mathrm{D}}{\mathrm{D}T}\zeta_{1z} + \frac{\mathrm{D}A}{\mathrm{D}\tau}\phi_{nz} = 0, \tag{3.2a}$$

$$\frac{\mathrm{D}u_1}{\mathrm{D}T} + \frac{1}{\rho_0} q_1 X - c_n \frac{\mathrm{D}A}{\mathrm{D}\tau}\phi_{nz} + c_n^2 A A_X\{\phi_{nz}^2 - \phi_n\phi_{nzz} - \beta N^2 \phi_n \phi_{nz}\} = 0, \tag{3.2b}$$

$$\frac{1}{\rho_0} q_{1z} + N^2\zeta_1 + c_n^2 A_{XX}\phi_n - \tfrac{1}{2}A^2 \frac{(\rho_0 N^2)_z}{\rho_0}\phi_n^2 = 0, \tag{3.2c}$$

$$\zeta_1 = g(X) \quad \text{on } z = 0, \tag{3.2d}$$

$$-\zeta_1 + \frac{\beta q_1}{\rho_0} + A^2\{-\phi_n\phi_{nz} - \tfrac{1}{2}\beta N^2 \phi_n^2\} = 0 \quad \text{on } z = h, \tag{3.2e}$$

where
$$\frac{\mathrm{D}}{\mathrm{D}\tau} = \frac{\partial}{\partial \tau} + \Delta \frac{\partial}{\partial X}. \tag{3.2f}$$

Here we note that $\mathrm{D}/\mathrm{D}T$ is defined by (2.8*e*) with V replaced by c_n. The solution of these equations is obtained by the same procedure described in §2 (compare (2.12*a–c*) and (2.13)). Thus we put

$$\zeta_1 = \sum_0^\infty A_{s1}(X, T; \tau)\, \phi_s(z), \tag{3.3a}$$

where
$$I_s A_{s1} = c_s^2 \int_0^h \rho_0 \zeta_{1z} \phi_{sz}\, \mathrm{d}z, \tag{3.3b}$$

with similar expressions for q_1 and u_1. We find that

$$\frac{1}{c_s^2} \frac{\mathrm{D}^2 A_{s1}}{\mathrm{D}T^2} = \frac{\partial^2 A_{s1}}{\partial X^2} + \frac{\partial^2 M_s}{\partial X^2}, \tag{3.4a}$$

where

$$I_s \frac{\partial M_s}{\partial X} = I_s \frac{\partial G_s}{\partial X} - \frac{2\delta_{sn} I_s}{c_n} \frac{\mathrm{D}A}{\mathrm{D}\tau} + A_{XXX} \int_0^h \rho_0 c_n^2 \phi_n \phi_s\, \mathrm{d}z$$
$$+ A A_X \int_0^h \rho_0 \phi_{sz} \{(c_n^2 + 2c_s^2)\, \phi_{nz}^2 + 2(c_s^2 - c_n^2)\, \phi_n \phi_{nzz}\}\, \mathrm{d}z. \tag{3.4b}$$

The solution of (3.4*a*) is analogous to the solution (2.16*a*) (or (2.17) and (2.18)) of (2.14*c*). Thus we find that

$$A_{s1} = -\frac{c_s^2}{(c_s^2 - c_n^2)} M_s(X; \tau) + \frac{c_s}{2c_s^+} M_s(X - c_s^+ T; \tau) + \frac{c_s}{2c_s^-} M_s(X + c_s^- T; \tau) \quad \text{if } c_s \neq c_n, \tag{3.5a}$$

or
$$A_{n1} = \tfrac{1}{2} c_n T M_{nX}(X; \tau) - \tfrac{1}{4}\{M_n(X; \tau) - M_n(X - 2c_n T; \tau)\} - \tfrac{1}{4}\{G_n(X) - G_n(X - 2c_n T)\}. \tag{3.5b}$$

Here we note that $c_s^\pm$ are defined by (2.16*b*) with V replaced by c_n. No other free long-wave terms have been included in (3.5*a*, *b*) in anticipation of the matching requirements described below. To avoid a secularity in A_{n1}, we must clearly put $M_n = 0$, which yields the amplitude equation

$$-\frac{1}{c_n}(A_\tau + \Delta A_x) + \mu A A_X + \lambda A_{XXX} + \tfrac{1}{2} G_{nX}(X) = 0, \tag{3.6a}$$

where
$$2I_n \mu = 3 \int_0^h \rho_0 c_n^2 \phi_{nz}^3\, \mathrm{d}z, \tag{3.6b}$$

$$2I_n \lambda = \int_0^h \rho_0 c_n^2 \phi_n^2\, \mathrm{d}z. \tag{3.6c}$$

Discussion of (3.6*a*) will be taken up in the next three sections.

It remains to be shown that the far-field expansion (3.1*a*) matches with the inner expansion (2.7). The matching conditions are obtained by substituting (3.1*b*) into (3.1*a*) and expanding in powers of $\alpha^{\frac{1}{2}}$, keeping X and T fixed. We find that

$$A(X, 0) = 0, \tag{3.7a}$$

$$A_\tau(X, 0) = \tfrac{1}{2} c_n G_{nX}(X). \tag{3.7b}$$

Here (3.7a) is deduced from the absence of any $\alpha^{\frac{1}{2}}$ term in (2.7), and (3.7b) then follows from (3.6a). Comparison with (2.18) as $T \to \infty$ shows that matching is achieved with the nth mode in the expansion (2.7). Also, using (3.7a), it follows that $M_s(X;0) = G_s(X)$ for $s \neq n$, and then (3.5a) matches with (2.17). Note that the free long-wave terms in (3.5a, b) are precisely those required by the matching procedure.

4. Discussion; analytic approximations for positive forcing

In this and the next two sections we shall discuss analytical and numerical solutions of the amplitude equation (3.6a), which can be recognized as a forced KdV equation, subject to the initial conditions (3.7a). First, let us rescale (3.6a) by putting

$$\tau^* = \lambda c_n \tau, \quad A^* = \frac{\mu}{6\lambda} A, \quad G^* = \frac{\mu}{12\lambda^2} G_n, \quad \Delta^* = \frac{\Delta}{\lambda c_n}. \tag{4.1}$$

The result is

$$-A^*_{\tau^*} - \Delta^* A^*_X + 6A^* A^*_X + A^*_{XXX} + G^*_X(X) = 0, \tag{4.2a}$$

$$A^*(X,0) = 0. \tag{4.2b}$$

Henceforth we shall omit the * in our discussion of (4.2a, b). Further, we shall consider only localized forcing functions $G(X)$, such that $G \to 0$ as $X \to \pm\infty$. The forcing function will be characterized by two parameters G_0 and ξ, where we put

$$G(X) = G_0 G'(X'), \tag{4.3}$$

where $X' = \xi X$. Here $G'(X') \geqslant 0$ for all X', has a maximum value of 1 at $X' = 0$, and $G' \to 0$ as $X' \to \pm\infty$. Thus G_0 is the maximum or minimum value of G according as G_0 is positive or negative. The positive parameter ξ measures the lengthscale of the forcing, i.e. ξ^{-1} is the half-width of the forcing. Equations (4.2a, b) were integrated numerically using the pseudospectral method of Fornberg & Whitham (1978). The forcing functions used were either

$$G'(X') = \operatorname{sech}^2 X', \tag{4.4a}$$

or

$$G'(X') = \exp(-X'^2). \tag{4.4b}$$

The results are shown in figures 4–13 and tables 1 and 2. These are discussed in detail in §5 for $G_0 > 0$ and again in §6 for $G_0 < 0$. For computational convenience, in the numerical solutions the forcing function was centred at $X = 85$. First, however, we shall present in this section some analytic approximate solutions to (4.2a, b) which are useful in interpreting the numerical solutions. These analytic approximations are not confined to the specific forcing functions (4.4a, b), and indicate that the response to the forcing functions (4.4a, b) is representative of the response to a wide class of forcing functions with similar shapes. In this section we consider the case $G_0 > 0$, which we call positive forcing. Because of the scaling (4.1), positive forcing corresponds to the case when the topography, and the solitary waves (see (4.7a, b) below) produced in the response to the forcing, have the same polarity.

For localized forcing we may assume that $A \to 0$ as $X \to \pm\infty$, for all $\tau \geqslant 0$. It then follows from (4.2a, b) that

$$\int_{-\infty}^{\infty} A(X,\tau)\,\mathrm{d}X = 0. \tag{4.5}$$

Indeed, interpreting the integral on the left-hand side of (4.5) as the mass, it is readily shown from (4.2*a*) that the mass is a constant, and then (4.2*b*) shows that the mass is zero. If we now define a potential B so that $A = B_X$, where, using (4.5), we may assume that $B \to 0$ is $X \to \pm\infty$, then it follows from (4.2*a*) that

$$-\frac{\partial}{\partial\tau}\int_{-\infty}^{\infty} B(X,\tau)\,\mathrm{d}X + \int_{-\infty}^{\infty} 3A^2(X,\tau)\,\mathrm{d}X + \int_{-\infty}^{\infty} G(X)\,\mathrm{d}X = 0. \tag{4.6}$$

Since the last two integrals in (4.6) are intrinsically positive, it follows that the first term cannot be zero, and hence the solution of (4.2*a*, *b*) is never stationary (i.e. independent of τ). This, of course, does not preclude the possibility of localized stationary solutions with non-zero mass, or of non-local stationary solutions (i.e. A approaches a non-zero constant as $X \to \pm\infty$).

In the absence of any forcing (i.e. $G(X) = 0$), (4.2*a*) has the well-known solitary-wave solutions

$$A = a\,\mathrm{sech}^2\, l(X - v\tau), \tag{4.7a}$$

where

$$\Delta - v = 2a = 4l^2. \tag{4.7b}$$

These are always waves of elevation ($a > 0$), with speeds $v < \Delta$. More generally, in the absence of forcing, (4.2*a*) has the periodic cnoidal wavetrain solution

$$A = a\{b(m) + \mathrm{cn}^2\,\gamma k(X - v\tau)\} + d, \tag{4.8a}$$

where

$$b(m) = \frac{1-m}{m} - \frac{E(m)}{mK(m)}, \tag{4.8b}$$

$$\Delta - v = 6d + 2a\left\{\frac{2-m}{m} - \frac{3E(m)}{mK(m)}\right\}, \tag{4.8c}$$

$$a = 2mk^2\gamma^2, \tag{4.8d}$$

$$\gamma\pi = K(m). \tag{4.8e}$$

Here cn is the Jacobian elliptic function of modulus m, while $K(m)$ and $E(m)$ are the complete elliptic integrals of the first and second kind respectively; the mean value of A over one period is d; the period has been defined so that the wavelength is $2\pi/k$. As $m \to 1$, $\mathrm{cn}^2(\ ) \to \mathrm{sech}^2(\ )$, $b(m) \to 0$, $\gamma \to \infty$ and $k \to 0$ with $l = k\gamma$ remaining finite; putting $d = 0$, we see that (4.8*a*) then reduces to the solitary-wave solution (4.7*a*, *b*). As $m \to 0$, $b + \mathrm{cn}^2(\ ) \to \cos 2(\ )$, $\gamma \to \frac{1}{2}$ and $a \to 0$ with $a/m \to \frac{1}{2}k^2$ and $v \to \Delta - 6d + k^2$; in this limit (4.8*a*) reduces to a sinusoidal wave train. We shall find that both these solutions (4.7*a*) and (4.8*a*) have a role to play in constructing analytical approximations.

A number of authors have recently discussed the forced KdV equation, both analytically and numerically. Patoine & Warn (1982), Warn & Brasnett (1983) and Malanotte-Rizzoli (1984) have all derived an equation of the form (4.2*a*) to describe the resonant forcing of Rossby waves by topography. Both Patoine & Warn (1982) and Malanotte-Rizzoli (1984) have discussed the existence of localized stationary solutions, and demonstrated the possibility of multiple solutions. It can be inferred from their results that localized stationary solutions exist for positive forcing ($G_0 > 0$) provided $|\Delta|$ is sufficiently large; for negative forcing ($G_0 < 0$) localized stationary solutions exist for all values of $|\Delta|$. However, our results indicate that these localized stationary solutions may not necessarily be realized, at least for the initial condition (4.2*b*), and, in any event, describe only a portion of the total

solution. Warn & Brasnett (1983) extend the analysis of Patoine & Warn (1982) to include the effects of linear damping. Patoine & Warn and Warn & Brasnett also discuss the case of solitary-wave capture by the forcing, i.e. the initial condition (4.2a) is replaced by a condition that allows a free solitary wave (4.7a) to propagate towards the localized forcing. Both Patoine & Warn and Malanotte-Rizzoli present some numerical solutions, the former for $\Delta < 0$, the latter for $\Delta = 0$ and both for negative forcing. A more comprehensive set of numerical solutions were obtained by Akylas (1984) and Cole (1985) for positive forcing, with, in our notation, G' given by a δ-function. Both these authors derived the forced KdV equation for the resonant forcing of water waves; Akylas considered a moving pressure distribution and Cole considered flow over bottom topography. Lee (1985) also derived a forced KdV equation for water waves due to either method of forcing, and made a detailed comparison between numerical solutions and experimental results for flow over a bottom bump. We shall discuss these numerical results later in §§5 and 6 in the context of our numerical results.

Various analytic approximations are possible. One approach is to search for localized stationary solutions; some aspects of this have been discussed above, and will be taken up again below in §4.2. Another possibility is to assume that $G_0 \ll 1$, and then seek a solution of (4.2a, b) in the form of an expansion in powers of G_0. This has been described in some detail by Patoine & Warn (1982). At the lowest order the equation to be solved is the linearized version of (4.2a), and the problem reduces to a simplified version of the flow of a stratified fluid over topography; for a comprehensive account of this latter problem, carried to terms of $O(G_0^2)$, see McIntyre (1972). In the present case, the solution to $O(G_0^2)$ obtained by Patoine & Warn can be summarized as follows. For $\Delta > 0$ (i.e. supercritical flow) the solution as $\tau \to \infty$ consists entirely of a localized stationary solution over the forcing region, together with a decaying oscillatory wavetrain which propagates downstream and is confined to the region $X > \Delta\tau$. For $\Delta < 0$ (i.e. subcritical flow), the solution as $\tau \to \infty$ consists of a localized stationary solution over the forcing region, together with a stationary, downstream lee wavetrain occupying the region $0 < X < -2\Delta\tau$. To $O(G_0)$ the wavetrain is described by (4.8a) with $d = 0$, $v = 0$ and wavenumber $k = (-\Delta)^{\frac{1}{2}}$; the corresponding group velocity is -2Δ, and defines the downstream extent of the wavetrain whose amplitude a_0 is proportional to $G_0\Delta^{-1}$. In addition there are $O(G_0^2)$ upstream and downstream disturbances; the upstream disturbance has a mean height of $-4|a_0|^2\Delta^{-1}(>0)$ and occupies the region $\Delta\tau < X < 0$, while the downstream disturbance has a mean height of $2|a_0|^2\Delta^{-1}(<0)$ and occupies the region $0 < X < 2\Delta\tau$. However, these approximate solutions would seem to be of limited value in interpreting our numerical results, as they are valid only for $G_0 \ll |\Delta|^2$. Indeed, near resonance, where $|\Delta|^2 \ll G_0$, our numerical results show that the solution has a very different character.

We shall base our analytic approximations upon the non-dispersive, or hydraulic, approximation in which the dispersive term (i.e. A_{XXX}) in (4.2a) is omitted. The primary motivation for this approach arises from examining our numerical results, but we note that Baines (1984), in an experimental and theoretical study of the flow of a two-layer fluid over topography, also found that the hydraulic approximation was of great utility in interpreting his experimental results. The hydraulic approximation will be discussed in §4.1 below. It is particularly useful in the forcing region, and so in §4.2 we discuss stationary solutions without necessarily invoking the hydraulic approximation. In the regions upstream and downstream from the forcing region the hydraulic approximation may lead to the prediction of shock formation.

However, the occurrence of shocks represents a failure of the hydraulic approximation, and hence they must be replaced by an appropriate solution of the full equation (4.2*a*). We find that these shocks must be replaced either by an upstream train of solitary waves, discussed in §4.3, or by a modulated cnoidal wave train, discussed in §4.4. Then in §§5 and 6 we shall present our numerical results and relate them to our analytic approximations.

4.1. *Hydraulic approximation*

This is formally valid for wide obstacles, in the limit $\xi \to 0$. Hence, if we assume that $A = A(X', \tau')$, where we recall from (4.3) that $X' = \xi X$ and we put $\tau' = \xi\tau$, then, with the omission of the dispersive term, which is $O(\xi^2)$, (4.2*a*, *b*) become

$$-A_{\tau'} - \Delta A_{X'} + 6AA_{X'} + G_{X'}(X') = 0, \tag{4.9a}$$

$$A(X', 0) = 0. \tag{4.9b}$$

These equations are readily solved by the method of characteristics. Thus we replace (4.9*a*, *b*) with

$$\frac{\mathrm{d}X'}{\mathrm{d}\tau'} = \Delta - 6A, \tag{4.10a}$$

$$\frac{\mathrm{d}A}{\mathrm{d}\tau'} = G_{X'}(X'), \tag{4.10b}$$

where

$$X' = X'_0, \quad A = 0 \quad \text{at } \tau' = 0. \tag{4.10c}$$

Here X'_0 is the initial position of the characteristic. The solution of (4.10*a*–*c*) is given by

$$6A = \Delta \mp \operatorname{sign} \Delta \{\Delta^2 + 12(G(X'_0) - G(X'))\}^{\frac{1}{2}} \tag{4.11}$$

Substitution of (4.11) into (4.10*a*) then gives X' as a function of X'_0 and τ'; elimination of X'_0 leads to the required solution. Here the upper sign in (4.11) is chosen until the characteristic reaches a turning point, where $\Delta = 6A$, after which the lower sign is chosen. When $\Delta = 0$ the upper sign is chosen in $X' > 0$ and the lower sign in $X' < 0$. If characteristics intersect, then a shock must be inserted. Letting V' be the shock velocity, it is readily shown from (4.9*a*) that the shock condition is

$$V' = \Delta - 3(A_1 + A_2), \tag{4.12}$$

where $A_{1,2}$ are the upstream and downstream values of A adjacent to the shock.

On constructing the solution by tracing characteristics in the manner described above, two distinct cases emerge. First, suppose that

$$\Delta^2 < 12G_0, \tag{4.13}$$

where we recall that $G_0 (> 0)$ is the maximum value of $G(X')$; we shall call this the resonant case. In this case there exists a critical value of X'_0, X'_{0c}, such that all characteristics emanating from X'_0 where $X'_0 < X'_{0c}$ have a turning point, propagate upstream and form an upstream shock; conversely all characteristics emanating from X'_0 where $X'_0 > X'_{0c}$ have no turning points, propagate downstream and form a downstream shock. A typical configuration is sketched in figure 2(*a*) for a case when $\Delta > 0$; the configuration for $\Delta < 0$ is similar (note that (4.9*a*) is invariant under the

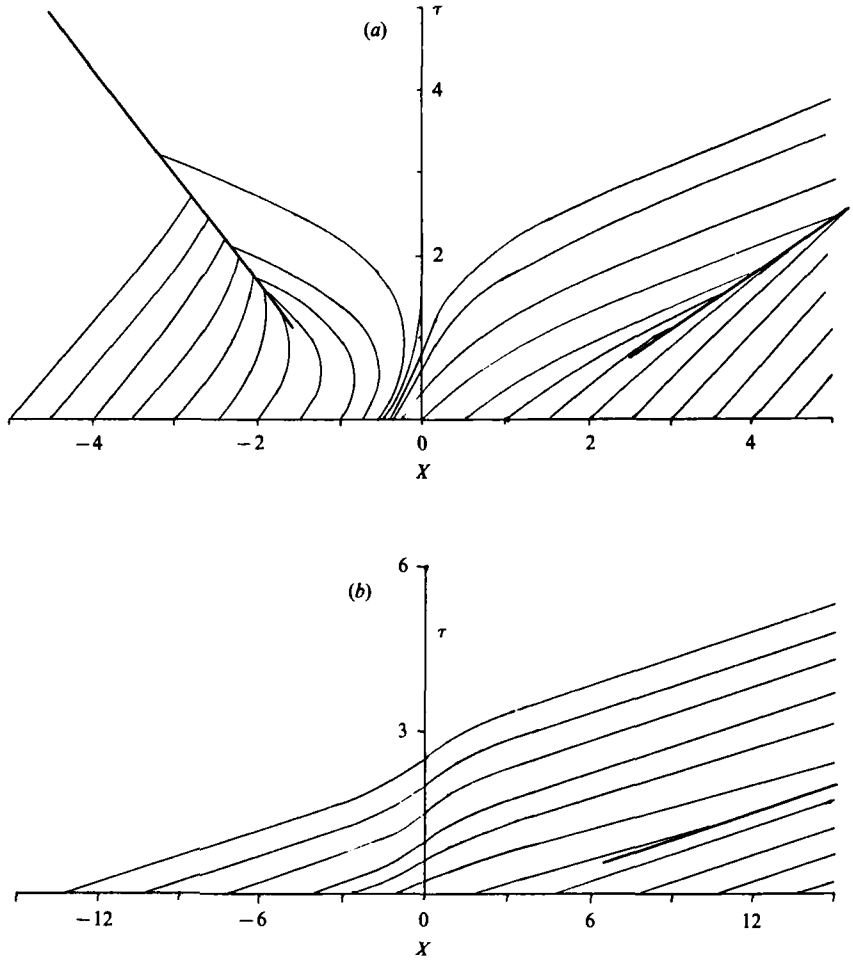

FIGURE 2. A typical characteristic configuration for the hydraulic approximation of §4.1 when $\Delta > 0$: (a) $\Delta^2 < 12G_0$; (b) $\Delta^2 > 12G_0$.

transformation $A \to -A$, $\Delta \to -\Delta$ and $X' \to -X'$). The critical value of X'_{0c} is given by

$$G(X'_{0c}) = G_0 - \tfrac{1}{12}\Delta^2, \tag{4.14}$$

where $X'_{0c} \lesseqgtr 0$ according as $\Delta \gtreqless 0$. For $\Delta = 0$, $X'_{0c} = 0$ and characteristics emanating from X'_0 where $X'_0 \lesseqgtr 0$ propagate upstream and downstream respectively. We are primarily interested in the asymptotic solution as $\tau' \to \infty$. In this limit a stationary solution develops over the forcing region terminating in upstream and downstream shocks. A typical configuration is sketched in figure 3(a) for a case $\Delta > 0$ (the configuration for $\Delta < 0$ is similar). The stationary solution is determined by the characteristic emanating from X'_{0c}, whose turning point is reached only as $\tau' \to \infty$; it is given by

$$6A_s = \Delta - \operatorname{sign} X'\{12(G_0 - G(X'))\}^{\frac{1}{2}}. \tag{4.15}$$

In hydraulic terminology the solution is determined by the critical condition $6A_s = \Delta$ at the top of the topography. As $X' \to \pm\infty$, $A_s \to A_\pm$ where from (4.15),

$$6A_\pm = \Delta \mp (12G_0)^{\frac{1}{2}}, \tag{4.16}$$

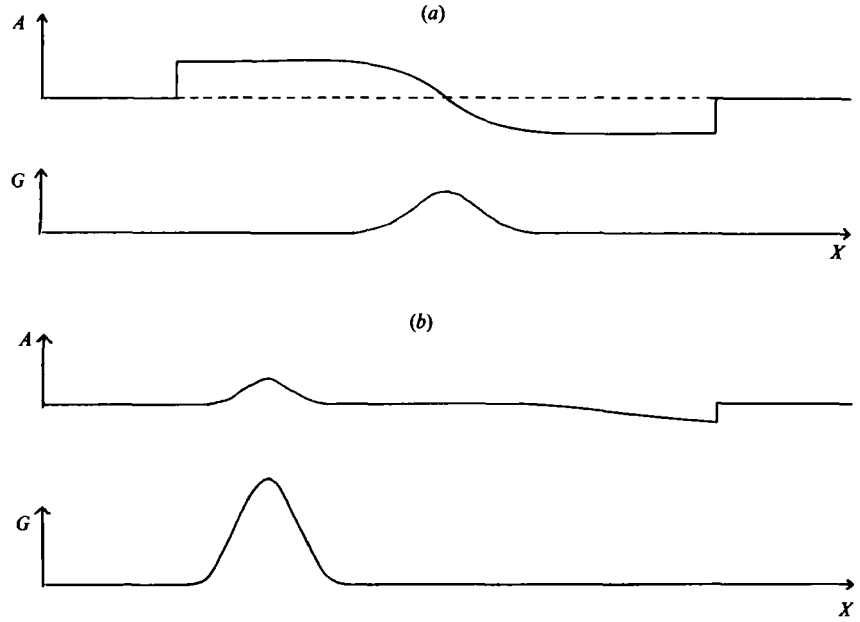

FIGURE 3. A typical solution as $\tau \to \infty$ for the hydraulic approximation of §4.1 when $\Delta > 0$: (a) $\Delta^2 < 12G_0$; (b) $\Delta^2 > 12G_0$.

while the corresponding shock velocities $V_\pm$ are found from (4.12), with the result that

$$V_\pm = \tfrac{1}{2}\{\Delta \pm (12G_0)^{\frac{1}{2}}\}. \tag{4.17}$$

Note that $V_\pm \gtrless 0$ respectively by virtue of the restriction (4.13), and $A_\pm \lesseqgtr 0$. As $\Delta \to (12G_0)^{\frac{1}{2}}$, $A_+ \to 0$, $V_+ \to (12G_0)^{\frac{1}{2}}$ and remains positive, while $A_- \to \frac{1}{3}(12G_0)^{\frac{1}{2}}$ and remains positive, $V_- \to 0$. Conversely, as $\Delta \to -(12G_0)^{\frac{1}{2}}$, $A_+ \to -\frac{1}{3}(12G_0)^{\frac{1}{2}}$ and remains negative, $V_+ \to 0$, while $A_- \to 0$, $V_- \to -(12G_0)^{\frac{1}{2}}$ and remains negative.

Next, suppose that

$$\Delta^2 > 12G_0, \tag{4.18}$$

which we shall call the non-resonant case. There are now no characteristics with turning points. For $\Delta > 0\,(< 0)$ all characteristics propagate downstream (upstream), and as $\tau' \to \infty$ a localized stationary solution develops over the forcing region, given by $A_s(X')$, where

$$6A_s = \Delta - \operatorname{sign}\Delta\{\Delta^2 - 12G(X')\}^{\frac{1}{2}}. \tag{4.19}$$

For $\Delta \gtrless 0$, $A_s \gtrless 0$, and as $X' \to \pm\infty$, $A_s \to 0$. However, in order to conserve mass (i.e. to satisfy (4.5)) there is a compensating simple wave and shock propagating downstream (upstream) for $\Delta > 0\,(< 0)$. A typical configuration for the characteristics is shown in figure 2(*b*), and a typical solution is sketched in figure 3(*b*). The solution has obvious similarities with the non-resonant solution obtained in §2. As $\tau' \to \infty$ the simple waves and shocks are given by the similarity solutions

$$6A \sim \Delta - \frac{X'}{\tau'} \quad \text{for } 0 < \left\{\frac{X'}{\tau'} - \Delta\right\} \operatorname{sign}\Delta < \frac{C}{(\tau')^{\frac{1}{2}}}, \tag{4.20a}$$

where

$$C^2 = 12 \operatorname{sign}\Delta \int_{-\infty}^{\infty} A_s(X')\,\mathrm{d}X'. \tag{4.20b}$$

They have the well-known triangular shape, terminating in a shock, and are negative (positive) according as $\Delta > 0\,(<0)$. Note that the integral on the right-hand side of (4.20*b*) is the mass contained in the localized stationary solution (4.19), and is exactly balanced by the mass contained in the asymptotic solution (4.20*a*).

4.2. *Stationary solutions*

In discussing the hydraulic approximation in §4.1, we found that the stationary solutions, (4.15) or (4.19), play a significant role in the limit $\tau \to \infty$. Hence in this subsection we shall develop some properties of the stationary solutions A_s of (4.2*a*) with the aim of extending the results obtained in §4.1, when $\xi \to 0$, to the whole range of ξ. We seek stationary solutions such that $A_s \to A_\pm$ as $X \to \pm\infty$. Two cases may be distinguished; based on the results of the hydraulic approximation, we conjecture that either

$$A_+ \neq A_-, \quad A_+ < 0 < A_- \quad \text{for } \Delta_-^{(1)} < \Delta < \Delta_+^{(1)}, \tag{4.21a}$$

or

$$A_+ = A_- = 0 \quad \text{for } \Delta < \Delta_-^{(2)} \text{ and } \Delta > \Delta_+^{(2)}. \tag{4.21b}$$

The relations (4.21*a*) hold for the resonant case, and (4.21*b*) for the non-resonant case; in both cases we anticipate that $\Delta_-^{(i)} < 0$ and $\Delta_+^{(i)} > 0$ $(i = 1, 2)$. In the resonant case (4.21*a*) the stationary solution must be matched to appropriate upstream and downstream transient wavetrains; in order that the total mass should be zero (see (4.5)) it is clear that A_+ and A_- should have opposite signs, and the requirement that $A_+ < 0 < A_-$ is based on the hydraulic approximation and the results obtained below. In the hydraulic approximation $\xi \to 0$ we have shown that $\Delta_\pm^{(i)} = \pm(12G_0)^{\frac{1}{2}}$ $(i = 1, 2)$, and $A_\pm$ are given by (4.16) with A_s given by (4.15) in the resonant case, and by (4.19) in the non-resonant case.

With no τ-dependence, (4.2*a*) may be integrated once to give

$$-\Delta A_s + 3A_s^2 + A_{sXX} + G = -3A_+ A_-, \tag{4.22a}$$

where

$$\Delta = 3(A_+ + A_-) \quad \text{if } A_+ \neq A_-. \tag{4.22b}$$

In the resonant case (4.21*a*) the following two integral identities may be derived from (4.22*a*, *b*).

$$3\int_{-\infty}^{\infty} (A_s - A_+)(A_s - A_-)\,\mathrm{d}X + \int_{-\infty}^{\infty} G\,\mathrm{d}X = 0, \tag{4.23a}$$

$$\tfrac{1}{2}(A_+ - A_-)^3 - \int_{-\infty}^{\infty} A_{sX} G\,\mathrm{d}X = 0. \tag{4.23b}$$

The hypothesis that $A_+ < A_s < A_-$ is consistent with both these identities, and is satisfied in the hydraulic approximation $\xi \to 0$. In the non-resonant case (4.21*b*) the corresponding integral identities are

$$-\Delta \int_{-\infty}^{\infty} A_s\,\mathrm{d}X + 3\int_{-\infty}^{\infty} A_s^2\,\mathrm{d}X + \int_{-\infty}^{\infty} G\,\mathrm{d}X = 0, \tag{4.24a}$$

$$\int_{-\infty}^{\infty} A_{sX} G\,\mathrm{d}X = 0. \tag{4.24b}$$

The hypothesis that $A_s \gtrless 0$ according as $\Delta > \Delta_+^{(2)} > 0$ or $\Delta < \Delta_-^{(2)} < 0$ is consistent with both these identities and is satisfied in the hydraulic approximation $\xi \to 0$.

Both Malanotte-Rizzoli (1984) and Patoine & Warn (1982) have discussed localized stationary solutions (i.e. (4.21*b*)) for the particular case when $G(X)$ is given by

$G_0 \operatorname{sech}^4 \xi X$; their results are consistent with the conjecture (4.21*b*), but indicate that there may be multiple solutions for A_s. To test these conjectures further, we consider the limit $\xi \to \infty$, and put

$$G = G_1 \delta(X), \tag{4.25}$$

where $G_1 > 0$. In order to provide a comparison with the hydraulic approximation, we note that (4.3) reduces to (4.25) in the limit $\xi \to \infty$ if we put

$$G_0 = G_1 \xi K^{-1}, \tag{4.26a}$$

where

$$K = \int_{-\infty}^{\infty} G'(X')\,\mathrm{d}X'. \tag{4.26b}$$

For the specific choices (4.4*a*, *b*), $K = 2, \pi^{\frac{1}{2}}$ respectively. In the resonant case (4.21*a*) the solution of (4.22*a*) with G given by (4.25) is

$$A_s = A_- \quad \text{for } X < 0, \tag{4.27a}$$

$$A_s = A_+ + 2l^2 \operatorname{sech}^2 l(X + X_1) \quad \text{for } X > 0, \tag{4.27b}$$

where

$$4l^2 = 3(A_- - A_+). \tag{4.27c}$$

The solution in $X > 0$ (4.27*b*) is a stationary solitary wave (see (4.7*a*, *b*)), and we note that there is no corresponding solitary wave in $X < 0$. To complete the solution, we must use the matching conditions at $X = 0$,

$$[A_s]^+_- = 0, \quad [A_{sX}]^+_- = -G_1, \tag{4.28}$$

and we find that

$$3 \operatorname{sech}^2 lX_1 = 2(A_- - A_+) \tag{4.29a}$$

$$(A_- - A_+)^3 = G_1^2. \tag{4.29b}$$

Note that (4.29*b*) can be deduced directly from (4.23*b*) using (4.28), and that only the positive solution for X_1 in (4.29*a*) is permissible. The two equations (4.22*b*) and (4.29*b*) determine $A_\pm$, and we find that

$$6A_\pm = \Delta \mp 3G_1^{\frac{2}{3}}, \tag{4.30a}$$

$$\Delta^{(1)}_\pm = \pm 3G_1^{\frac{2}{3}}. \tag{4.30b}$$

In the non-resonant case the solution is

$$A_s = 2l^2 \operatorname{sech}^2 l(X \pm X_1) \quad \text{for } X \gtrless 0, \tag{4.31a}$$

where

$$4l^2 = \Delta. \tag{4.31b}$$

The matching conditions at $X = 0$ imply that

$$\operatorname{sech}^2(lX_1) \tanh lX_1 = G_1 \Delta^{-\frac{3}{2}}. \tag{4.32}$$

The solution exists only for $\Delta > 0$ and for $G_1 \Delta^{-\frac{3}{2}} < 2/3^{\frac{3}{2}}$. We deduce that

$$\Delta^{(2)}_+ = 3(\tfrac{1}{2}G_1)^{\frac{2}{3}}, \quad \Delta^{(2)}_- \to -\infty. \tag{4.33}$$

Note that there are two allowed solutions for X_1 when solving (4.32), and hence two solutions for A_s. The two solutions are such that $\tanh lX_1 \gtrless 3^{-\frac{1}{2}}$ respectively; considering the limit $\Delta \to \infty$, it is clear that we should select the larger solution. For $\Delta < -3G_1^{\frac{2}{3}}$ there is no stationary solution of either kind; our numerical results and some analysis for $G_0 \ll 1$ by Patoine & Warn (1982) suggest that when Δ is sufficiently negative there is a quasistationary solution consisting of a downstream stationary

cnoidal wavetrain (i.e. (4.8*a–e*) with $v = 0$) and an upstream constant, A_-; both upstream and downstream components must be matched to appropriate transient wavetrains.

4.3. *Solitary wavetrain*

In our discussion of stationary solutions in §4.2 we have shown that in the resonant case (4.21*a*) a mean level $A_- > 0$ is established in the upstream region where $X < X_- < 0$, where, for simplicity, we shall assume that G is effectively zero in $X < X_-$. In the hydraulic approximation (§4.1) the mean level A_- is terminated by a shock travelling upstream with a velocity V_- (see (4.16) and (4.17)). However, shocks are not valid solutions of the free KdV equation (i.e. (4.2*a*) with the forcing term omitted); indeed, the hypotheses that lead to the hydraulic approximation fail in the vicinity of the shock. Instead, motivated by our numerical results, we propose that the mean level A_- generates a train of identical solitary waves propagating upstream.

It is well known that an initial positive disturbance for the free KdV equation in the infinite interval $-\infty < X < \infty$ will generate a finite number of amplitude-ordered solitary waves, together with a decaying oscillatory wavetrain (see e.g. Whitham 1974). The present situation is different in that we are seeking solutions of the free KdV equation in the semi-infinite interval $-\infty < X < X_-$, with a zero initial condition, and a positive disturbance as $X \to X_-$. We shall view the boundary condition at X_- as providing a continual flux of mass and energy, with the consequent formation of a series of identical solitary waves, with amplitude a and speed v and given by (4.7*a*, *b*). The spacing between the waves is h, and in the limit $\tau \to \infty$ the number N of solitary waves produced is given by $N \sim -v\tau h^{-1}$. Strictly speaking, a train of identical solitary waves is not an exact solution of the free KdV equation, and a more accurate representation is a modulated cnoidal wavetrain. This is described locally by (4.8*a–e*) with the parameters a, m and d varying slowly with X and τ. The general theory has been developed by Whitham (1965, 1974) and applied by one of us (Smyth 1986) to the present problem (see also §4.4). It is found that the modulus m varies in the range $0 < m_0 \leqslant m \leqslant 1$, where $m \to 1$ at the upstream front of the wavetrain, and $m \to m_0$ in the forcing region (i.e. as $X \to X_-$). Thus the leading waves are closely approximated by a train of solitary waves. Furthermore, for much of the range of Δ where this solution applies, Smyth (1986) also finds that m_0 is sufficiently close to 1 for the whole wavetrain to be adequately described as a solitary wavetrain. Hence we shall proceed on this basis here.

In order to apply the boundary condition as $X \to X_-$ we observe that the following conservation laws for mass and energy can be derived from the KdV equation (4.2*a*)

$$\frac{\partial}{\partial \tau} \int_{-\infty}^{X_0} A \, \mathrm{d}X = \{-\Delta A + 3A^2 + A_{XX} + G\}_{X_0}, \tag{4.34a}$$

$$\frac{\partial}{\partial \tau} \int_{-\infty}^{X_0} \tfrac{1}{2} A^2 \, \mathrm{d}X = \{-\tfrac{1}{2}\Delta A^2 + 2A^3 + AA_{XX} - \tfrac{1}{2}A_X^2\}_{X_0} + \int_{-\infty}^{X_0} AG_X \, \mathrm{d}X. \tag{4.34b}$$

These expressions are valid for arbitrary fixed values of X_0. Here we choose X_0 to lie in the region where the solution is stationary, i.e. $A = A_s(X)$ and is given by (4.22*a*, *b*). We find that (4.34*a*, *b*) become

$$\frac{\partial}{\partial \tau} \int_{-\infty}^{X_0} A \, \mathrm{d}X = -\Delta A_- + 3A_-^2, \tag{4.35a}$$

$$\frac{\partial}{\partial \tau} \int_{-\infty}^{X_0} \tfrac{1}{2} A^2 \, \mathrm{d}X = -\tfrac{1}{2}\Delta A_-^2 + 2A_-^3. \tag{4.35b}$$

The mass and energy carried by a single solitary wave are $2(2a)^{\frac{1}{2}}$ and $\frac{1}{3}(2a)^{\frac{3}{2}}$ respectively. For a train of N solitary waves, where $N \sim -v\tau h^{-1}$, the left-hand sides of (4.35a, b) can be evaluated to give

$$-\frac{v}{h}.2(2a)^{\frac{1}{2}} = -\Delta A_- + 3A_-^2, \tag{4.36a}$$

$$-\frac{v}{h}.\frac{(2a)^{\frac{3}{2}}}{3} = -\tfrac{1}{2}\Delta A_-^2 + 2A_-^3. \tag{4.36b}$$

Recalling the relation (4.7b) between v and a, we find that

$$a = \frac{3A_-(4A_- - \Delta)}{2(3A_- - \Delta)}, \tag{4.37a}$$

$$v = -\frac{(3A_- - \Delta)^2 + 3A_-^2}{3A_- - \Delta}, \tag{4.37b}$$

and h can be found from (4.36a, b). Recalling (4.22b), we see that $3A_- - \Delta > 0$ and hence $a > 0$, $v < 0$ and $h > 0$, as required for solitary waves.

In the hydraulic approximation (§4.1) A_- is given by (4.16), and (4.37a) becomes

$$a \approx \frac{(12G_0)^{\frac{1}{2}} + \Delta}{(12G_0)^{\frac{1}{2}} - \Delta}\{\tfrac{1}{3}(12G_0)^{\frac{1}{2}} - \tfrac{1}{6}\Delta\} \quad \text{as } \xi \to 0, \quad \text{for } |\Delta| < (12G_0)^{\frac{1}{2}}. \tag{4.38}$$

As $\Delta \to (12G_0)^{\frac{1}{2}}$, a and $h \to \infty$, although, in this limit, the time for the solution to reach the asymptotic regime of a solitary wavetrain increases indefinitely, with the consequence that formulae such as (4.38) become less useful. As $\Delta \to -(12G_0)^{\frac{1}{2}}$, $a \to 0$ and $h \to \infty$; however, we shall show in §4.4 that for $\Delta < -\frac{1}{2}(12G_0)^{\frac{1}{2}}$ the solitary wavetrain is replaced by a modulated cnoidal wavetrain. In the opposite approximation, $\xi \to \infty$, A_- is given by (4.30a), where G_1 is given by (4.26a, b). We find that (4.37a) becomes

$$a \approx \frac{3(G_0 K\xi^{-1})^{\frac{2}{3}} + \Delta}{3(G_0 K\xi^{-1})^{\frac{2}{3}} - \Delta}\{(G_0 K\xi^{-1})^{\frac{2}{3}} - \tfrac{1}{6}\Delta\} \quad \text{as } \xi \to \infty, \quad \text{for } |\Delta| < 3(G_0 K\xi^{-1})^{\frac{2}{3}}. \tag{4.39}$$

Similar comments to those made above hold when $|\Delta| \to 3(G_0 K\xi^{-1})^{\frac{2}{3}}$. We shall find that (4.38) and (4.39) together provide a useful approximation to the amplitude of the upstream solitary waves for all values of ξ.

4.4. *Modulated cnoidal wavetrain*

In our discussion of stationary solutions in §4.2 we have shown that in the resonant case (4.21a) a mean level $A_+ < 0$ is established in the downstream region $X > X_+ > 0$ where, for simplicity, we shall assume that G is effectively zero in $X > X_+$. In the hydraulic approximation (§4.1) the mean level A_+ is terminated by a downstream shock (see (4.16) and (4.17)). However, since shocks are not valid solutions of the free KdV equation, we shall instead terminate the mean level with a modulated cnoidal wavetrain. The relevant approximate solution has been described by Gurevich & Pitaevskii (1974) and Fornberg & Whitham (1978), based on the modulation theory developed by Whitham (1965, 1974). More details relating to the present application are given by Smyth (1986). The modulated wavetrain is described by the cnoidal wavetrain (4.8a–e), where the parameters a, m and d vary slowly with X and τ. The

solution that describes the transition from a mean level $A_+ < 0$ to a zero mean level is given by (4.8*a–e*), where

$$\Delta - \frac{X}{\tau} = 2A_+\left\{2-m+\frac{2m(1-m)\,K(m)}{E(m)-(1-m)\,K(m)}\right\} \quad \text{for } \Delta - 2A_+ < \frac{X}{\tau} < \Delta - 12A_+, \tag{4.40a}$$

$$a = -2A_+ m, \tag{4.40b}$$

$$d = A_+\left\{2-m-\frac{2E(m)}{K(m)}\right\}. \tag{4.40c}$$

Ahead of the wavetrain, where $X/\tau > \Delta - 12A_+$, $A = 0$ and at this end $m \to 0$, $a \to 0$, $d \to 0$ and the wavetrain is approximately sinusoidal. Behind the wavetrain, where $X/\tau < \Delta - 2A_+$, $A = A_+$ and at this end $m \to 1$, $a \to -2A_+$, $d \to A_+$ and the leading wave is approximately a solitary wave of amplitude $-2A_+$. In order that this solution lie in the region $X > 0$, we require that

$$2A_+ < \Delta. \tag{4.41}$$

In the hydraulic approximation (§4.1) A_+ is given by (4.16), and the modulated wavetrain occupies the region

$$\tfrac{2}{3}\Delta + \tfrac{1}{3}(12G_0)^{\frac{1}{2}} < \frac{X}{\tau} < 2(12G_0)^{\frac{1}{2}} - \Delta \quad \text{as } \xi \to 0, \tag{4.42a}$$

where

$$-\tfrac{1}{2}(12G_0)^{\frac{1}{2}} < \Delta < (12G_0)^{\frac{1}{2}}. \tag{4.42b}$$

Here the upper limit in (4.42*b*) derives from the condition (4.13) for the resonant case, but the lower limit is due to (4.41). In the opposite approximation $\xi \to \infty$, A_+ is given by (4.30*a*), where G_1 is given by (4.26*a*, *b*). The wavetrain now occupies the region

$$\tfrac{2}{3}\Delta + (G_0 K\xi^{-1})^{\frac{2}{3}} < \frac{X}{\tau} < 6(G_0 K\xi^{-1})^{\frac{2}{3}} - \Delta \quad \text{as } \xi \to \infty, \tag{4.43a}$$

where

$$-\tfrac{3}{2}(G_0 K\xi^{-1})^{\frac{2}{3}} < \Delta < 3(G_0 K\xi^{-1})^{\frac{2}{3}}. \tag{4.43b}$$

In (4.43*b*) the upper limit is due to (4.30*b*), and the lower limit is due to (4.41). We shall find that (4.40*a–c*), (4.42*a*, *b*) and (4.43*a*, *b*) together provide a useful description of the downstream oscillatory wavetrain for all values of ξ. When the condition (4.41) is violated, the solution (4.40*a–c*) is replaced by a stationary cnoidal wavetrain with constant modulus $m_s\,(< 1)$ in the region $X_+ < X < X_1\tau$ and by the similarity solution (4.40*a*, *b*, *c*) in the region $X_1\tau < X < (\Delta - 12A_+)\tau$, and for which $m_s > m > 0$. Details of this solution and the determination of m_s and X_1 are given by Smyth (1986), who also shows that this solution pertains for $-(12G_0)^{\frac{1}{2}} < \Delta < -\frac{1}{2}(12G_0)^{\frac{1}{2}}$ when $\xi \to 0$, and for $-3(G_0 K\xi^{-1})^{\frac{2}{3}} < \Delta < -\frac{3}{2}(G_0 K\xi^{-1})^{\frac{2}{3}}$ when $\xi \to \infty$.

It is also possible to use a modulated cnoidal wavetrain to terminate the upstream mean level $A_- > 0$ in the region $X < X_- < 0$ instead of the solitary wavetrain described in §4.3. The solution is given by (4.8*a–e*) where now

$$\Delta - \frac{X}{\tau} = 2A_-\left\{(1+m)-\frac{2m(1-m)\,K(m)}{E(m)-(1-m)\,K(m)}\right\} \quad \text{for } \Delta - 4A_- < \frac{X}{\tau} < \Delta + 6A_-, \tag{4.44a}$$

$$a = 2A_- m, \tag{4.44b}$$

$$d = A_-\left\{m-1+\frac{2E(m)}{K(m)}\right\}. \tag{4.44c}$$

Ahead of the wavetrain, $X/\tau < \Delta - 4A_-$, $A = 0$ and at this end $m \to 1$, $a \to 2A_-$, $d \to 0$ and the leading wave is a solitary wave of amplitude $2A_-$. Behind the wavetrain, $X/\tau > \Delta + 6A_-$, $A = A_-$ and at this end $m \to 0$, $a \to 0$, $d \to A_-$ and the wavetrain is approximately sinusoidal. In order that this solution lie in the region $X < 0$ we require that

$$6A_- < -\Delta. \tag{4.45}$$

In the hydraulic approximation (§4.1) A_- is given by (4.16), and the modulated wavetrain occupies the region

$$\tfrac{1}{3}\Delta - \tfrac{2}{3}(12G_0)^{\frac{1}{2}} < \frac{X}{\tau} < 2\Delta + (12G_0)^{\frac{1}{2}} \quad \text{as } \xi \to 0, \tag{4.46a}$$

where

$$-(12G_0)^{\frac{1}{2}} < \Delta < -\tfrac{1}{2}(12G_0)^{\frac{1}{2}}. \tag{4.46b}$$

Here the upper limit in (4.46*b*) is due to (4.45), but the lower limit derives from the condition (4.13) for the resonant case. In the opposite approximation $\xi \to \infty$, A_- is given by (4.30*a*), where G_1 is given by (4.26*a*, *b*). The wavetrain now occupies the region

$$\tfrac{1}{3}\Delta - 2(G_0 K \xi^{-1})^{\frac{2}{3}} < \frac{X}{\tau} < 2\Delta + 3(G_0 K \xi^{-1})^{\frac{2}{3}} \quad \text{as } \xi \to \infty, \tag{4.47a}$$

where

$$-3(G_0 K \xi^{-1})^{\frac{2}{3}} < \Delta < -\tfrac{3}{2}(G_0 K \xi^{-1})^{\frac{2}{3}}. \tag{4.47b}$$

In (4.47*b*) the upper limit is due to (4.45), and the lower limit is due to (4.30*b*). When the condition (4.45) is violated, we shall use the solitary-wavetrain approximation of §4.3. However, as we commented there, a more accurate approximation is to use the similarity solution (4.44*a*–*c*) in the region $(\Delta - 4A_-)\tau < X < X_-$, and for which $1 > m > m_0$. Details of this solution, and the determination of m_0, are given by Smyth (1986), who also shows that this solution pertains for $-\frac{1}{2}(12G_0)^{\frac{1}{2}} < \Delta < (12G_0)^{\frac{1}{2}}$ when $\xi \to 0$, and for $-\frac{3}{2}(G_0 K \xi^{-1})^{\frac{2}{3}} < \Delta < 3(G_0 K \xi^{-1})^{\frac{2}{3}}$ when $\xi \to \infty$.

5. Discussion; numerical solutions for positive forcing

In this section we shall discuss the numerical solutions of (4.2*a*, *b*) obtained using the forcing functions (4.4*a*, *b*) with $G_0 > 0$. Synthesizing our numerical results with the aid of the analytic approximations obtained in §4, we postulate the existence of four regimes.

5.1. *Case* (*i*): $\Delta_- < \Delta < \Delta_+$

This is the resonant case. Here $\Delta_\pm$ are functions of G_0 and ξ, and satisfy the inequality $\Delta_-^{(1)} \leqslant \Delta_- < 0 < \Delta_+ \leqslant \Delta_+^{(1)}$, where $\Delta_\pm^{(1)}$ are defined in (4.21). In the limit $\tau \to \infty$ the solution becomes locally stationary in the forcing region, where it is given by A_s, and we recall from §4.2 that $A_s \to A_\pm$ as $X \to \pm\infty$, where $A_+ < 0 < A_-$ (see (4.21*a*)). Upstream, the mean level A_- is matched to a train of solitary waves of uniform amplitude. We have discussed these in §4.3, and we recall the approximate expressions (4.37*a*, *b*) for the solitary waves' amplitude and speed. Downstream, the mean level A_+ is matched to a modulated cnoidal wavetrain, discussed in §4.4 (see (4.40*a*–*c*). In the hydraulic approximation $\xi \to 0$ our analytic approximations obtained in §4 show that $\Delta_- \approx -\frac{1}{2}(12G_0)^{\frac{1}{2}}$ and $\Delta_+ \approx (12G_0)^{\frac{1}{2}}$ (see e.g. (4.42*b*)). The solitary-wave amplitudes are given by (4.38), and the downstream modulated cnoidal wavetrain occupies the region given by (4.42*a*). In the opposite limit $\xi \to \infty$,

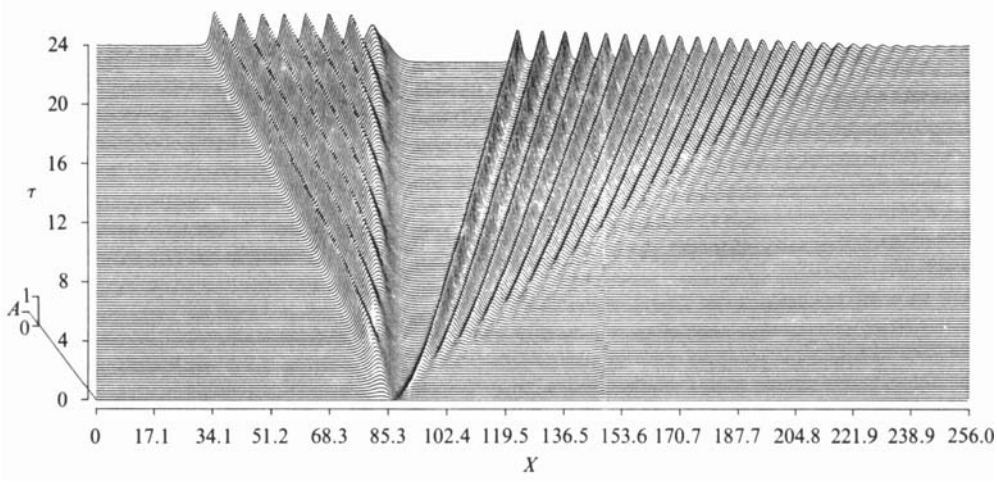

FIGURE 4. The numerical solution for the forcing function (4.4a) with $\Delta = 0$, $G_0 = 1$ and $\xi = 0.3$.

$\Delta_- \approx -\frac{3}{2}(G_0 K\xi^{-1})^{\frac{2}{3}}$ and $\Delta_+ \approx 3(G_0 K\xi^{-1})^{\frac{2}{3}}$ (see e.g. (4.43b)), where K is defined by (4.26b). The solitary wave amplitudes are given by (4.39), and the downstream modulated cnoidal wavetrain occupies the region given by (4.43a).

A typical numerical solution is shown in figure 4 for the forcing function (4.4a) with $\Delta = 0$, $G_0 = 1$ and $\xi = 0.3$. The general features described above are clearly apparent. With Δ in the range $\Delta_- < \Delta < \Delta_+$ we find that varying G_0, ξ or the forcing function (4.4a, b) makes little qualitative difference to our numerical solutions, in agreement with the discussion in the previous paragraph. Here $\Delta_\pm$ are found from interpreting our numerical solutions. For instance, with $G_0 = 1$, $\xi = 0.3$ and the forcing function (4.2a), we find $\Delta_- \approx -1.7$ and $\Delta_+ \approx 3.3$, in good agreement with the predictions of the hydraulic approximation, $\Delta_- \approx -\sqrt{3}$, $\Delta_+ \approx 2\sqrt{3}$. For $\xi \ll 1$ the numerical solutions obtained with either of the forcing functions (4.4a, b) are quantitatively in agreement. This is a consequence of the hydraulic approximation in which the stationary solution in the forcing region, and hence $A_\pm$, the upstream solitary wavetrain and the downstream modulated cnoidal wavetrain, are all functions only of G_0 and Δ. For moderate or large values of ξ the numerical solutions are qualitatively the same. For $\xi \gg 1$ the discussion in §4.2 indicates that the solution is determined by the parameters $G_0 K\xi^{-1}$ and Δ.

In table 1 we compare the numerically calculated solitary wave amplitude a and the downstream depression A_+ with the approximate expressions (4.38) and (4.16) respectively, which are valid in the limit $\xi \to 0$. The numerical solutions are obtained for the forcing function (4.4a) with $\Delta = 0$, $\xi = 0.3$ and a range of values for G_0. The agreement is good. In figure 5 we plot the numerically calculated solitary-wave amplitude a and the downstream depression A_+ as functions of ξ, for the forcing function (4.4b) with $\Delta = 0$ and $G_0 = 1$. Also shown are the approximate expressions (4.38) for a and (4.16) for A_+ that hold in the limit $\xi \to 0$, and the approximate expressions (4.39) for a and (4.30a) for A_+ that hold in the limit $\xi \to \infty$. The approximations (4.38) and (4.16) derive from the hydraulic approximation and predict that both a and A_+ are independent of ξ; our numerical results show that this is a very good approximation for $\xi > 1$. In contrast, the approximations (4.39) and (4.30a) derive from the limit $\xi \to \infty$ and predict that both a and A_- are

G_0	a, numerical	a, approximate	$\lvert A_+\rvert$, numerical	$\lvert A_+\rvert$, approximate
0.5	0.81	0.82	0.400	0.408
1.0	1.15	1.15	0.577	0.577
1.5	1.41	1.41	0.707	0.707
2.0	1.61	1.63	0.817	0.817

TABLE 1. A comparison between the numerically calculated results for the solitary-wave amplitude a and the downstream depression A_+, and the approximate expressions that hold as $\xi \to 0$. The numerical results were obtained for the forcing function (4.4a) with $\Delta = 0$ and $\xi = 0.3$.

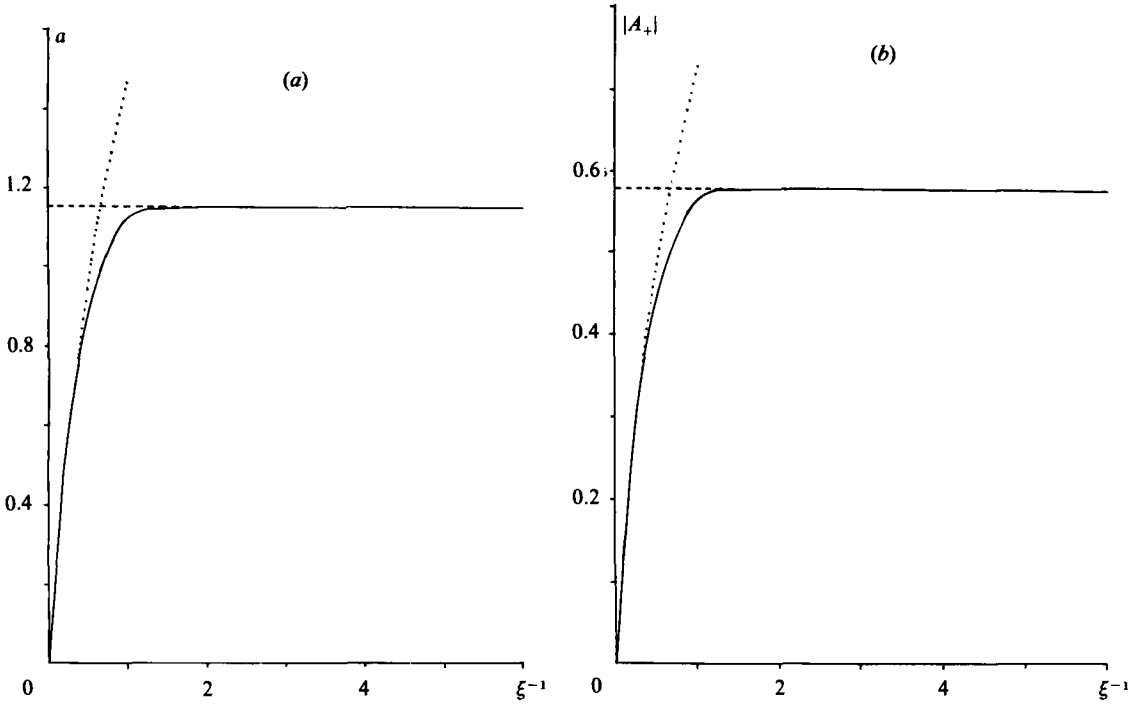

FIGURE 5. A comparison between the numerically calculated results (——) as a function of ξ and the approximate expressions that hold as $\xi \to 0$ (– – – –) or as $\xi \to \infty$ (...): (a) the solitary wave amplitude a; (b) the downstream depression A_+. The numerical results were obtained for the forcing function (4.4b) with $\Delta = 0$ and $G_0 = 1$.

proportional to $\xi^{-\frac{2}{3}}$; our numerical results show that this is a very good approximation for $\xi < 1$. Taken together, the two limits $\xi \to 0$ and $\xi \to \infty$ provide good approximate expressions for a and A_+ over the whole range of ξ. Next we turn to the downstream wavetrain. Our numerical solutions provide clear evidence that this can be described by the modulated cnoidal wavetrain approximation discussed in §4.4. For instance, examination of figure 4 shows clear evidence that the crest positions are functions of the similarity variable X/T. In table 2 we compare the numerically calculated positions of the ends of this wavetrain with the approximate expressions (4.42a), which are valid in the limit $\xi \to 0$. The numerical solutions are obtained for the forcing function (4.4a) with $\Delta = 0$, $\xi = 0.3$ and a range of values of G_0. There is good agreement for the lower limit, where the leading wave is close to a solitary wave and clearly defined. The agreement with the upper limit is reasonable, but not so good.

G_0	Numerical results	Approximate results
0.5	$0.82 < X/\tau < 5.75$	$0.82 < X/\tau < 4.90$
1.0	$1.16 < X/\tau < 7.45$	$1.15 < X/\tau < 6.93$
1.5	$1.41 < X/\tau < 9.44$	$1.41 < X/\tau < 8.49$
2.0	$1.62 < X/\tau < 9.94$	$1.63 < X/\tau < 9.80$

TABLE 2. A comparison between the numerically calculated results for the ends of the downstream wavetrain, and the approximate expressions that hold as $\xi \to 0$. The numerical results were obtained for the forcing function (4.4a) with $\Delta = 0$ and $\xi = 0.3$.

However, we note that the numerical results of Fornberg & Whitham (1978) show that the modulation theory, described here in §4.4, generally underestimates the upper limit.

Next we examine how the comparison between the numerical solutions and the analytic approximations fare as a function of Δ. In figure 6 we plot the numerically calculated solitary wave amplitude a and the downstream depression A_+ as functions of Δ, for the forcing function (4.4b) with $G_0 = 1$ and $\xi = 0.3$. For this value of ξ the approximations (4.38) for a, and (4.16) for A_+, derived from the hydraulic approximation, may be used, and are also shown in figure 6. In this same approximation $\Delta_- \approx -\frac{1}{2}(12G_0)^{\frac{1}{2}}$ and $\Delta_+ \approx (12G_0)^{\frac{1}{2}}$. There is good agreement for A_+ over the whole range of Δ, and reasonably good agreement for a over most of the range Δ. The major disagreement occurs in the approximation for a as $\Delta \to \Delta_+$. This is due in part to an increase in the time taken for the asymptotic regime of an upstream solitary wavetrain to be established with the consequent difficulty of determining the amplitude a. A contributing factor is that as $\Delta \to \Delta_+$, $A_+ \to 0$ and the mass flux being supplied to the upstream wavetrain also tends to zero (see (4.35a), and use (4.22b)). This has the consequence that the hypothesis of a solitary wavetrain as the asymptotic regime becomes less useful as $\Delta \to \Delta_+$. One of us (Smyth 1986) has replaced the solitary-wavetrain approximation with a modulated cnoidal wavetrain whose modulus m varies from m_0 just upstream of the forcing region to 1 at the upstream front of the wavetrain. He finds that the amplitude of the leading wave, which is closely approximated by a solitary wave, varies with Δ in a manner that is completely consistent with our numerical results for the whole range $\Delta_- < \Delta < \Delta_+$. A typical numerical solution when Δ is just less than Δ_+ is shown in figure 7 for the forcing function (4.4a) with $\Delta = 3$, $G_0 = 1$ and $\xi = 0.3$; here $\Delta_+ \approx 3.3$.

Finally we compare our numerical and analytical solutions with the numerical solutions obtained by Akylas (1984), Cole (1985) and Lee (1985). Both Akylas and Cole numerically integrated (4.2a, b) when G is given by a δ-function; in our notation $G_1 = (\frac{4}{3})^{\frac{1}{2}}\pi$ or $\frac{1}{2}(\frac{3}{4})^{\frac{2}{3}}$ for the results of Akylas and Cole respectively. The appropriate analytical approximations for $\Delta_\pm$ are those that hold in the limit $\xi \to \infty$, and we find that $\Delta_+ = 6.86$ and $\Delta_- = -3.43$ for the results of Akylas, while $\Delta_+ = 1.66$ and $\Delta_- = -0.83$ for the results of Cole. Akylas describes results for (in our notation) $\Delta = 0$, 0.45 and -0.91, which thus all fall well within our resonant category $\Delta_- < \Delta < \Delta_+$. In general his numerical results conform with the description given here. For the three values of Δ reported by Akylas, our analytical approximations for the solitary-wave amplitude (4.39) and the downstream depression (4.30a) are $a = 2.29$, 2.52 and 1.87 and $A_+ = -1.14$, -1.07 and -1.29 respectively. These compare with $a = 1.82$, 2.06 and 1.47 and $A_+ = -0.98$, -0.81 and -1.10 respectively obtained by Akylas. We suspect that the reason for the discrepancy is that the

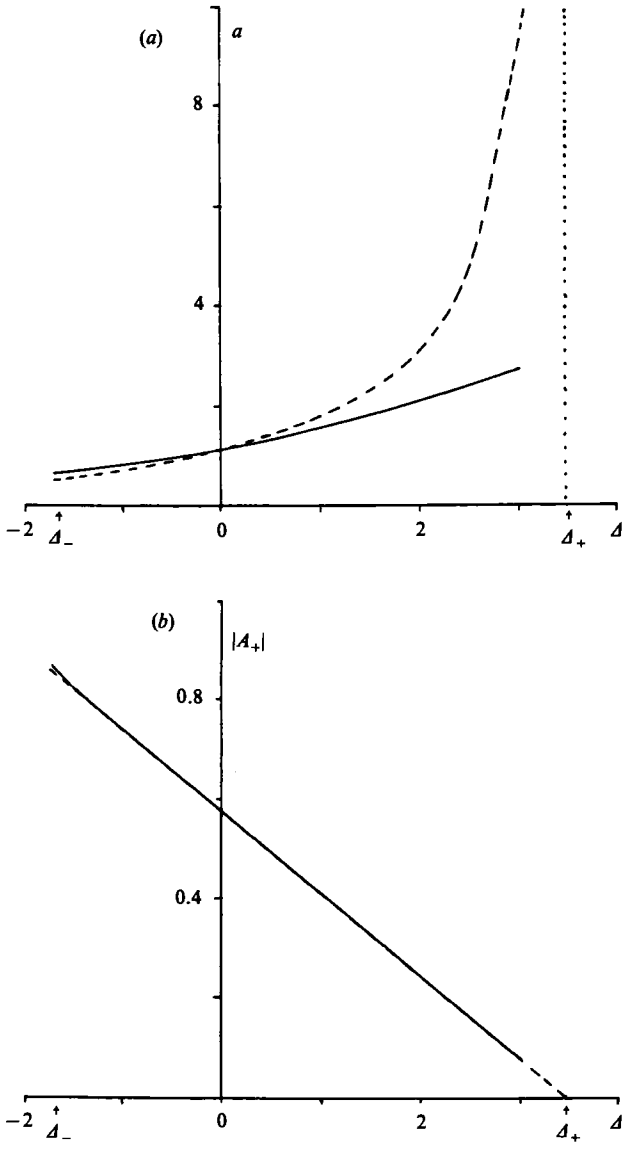

FIGURE 6. A comparison between the numerically calculated results (——) as a function of Δ and the approximate expressions that hold as $\xi \to 0$ (– – –); (*a*) the solitary wave amplitude a; (*b*) the downstream depression A_+. The numerical results were obtained for the forcing function (4.4*b*) with $G_0 = 1$ and $\xi = 0.3$.

numerical calculations obtained by Akylas were terminated before the asymptotic regime had been completely established. As a further comparison, we obtained a numerical solution for the forcing function (4.4*b*) with $\Delta = 0$, $\xi = 7.0$ and G_0 given by (4.26*a*), and found that our numerically determined solitary wave amplitude and downstream depression were $a = 2.27$ and $A_+ = -1.12$, in good agreement with our analytical approximations. Next, Cole describes results for (in our notation) $\Delta = 0.91$, 0.45, 0, −0.45 and −0.91; the first four of these cases fall within our resonant category (i), while the last belongs to our transition category (ii) (see §5.2). In general, her numerical results conform with the description given here, but no quantitative

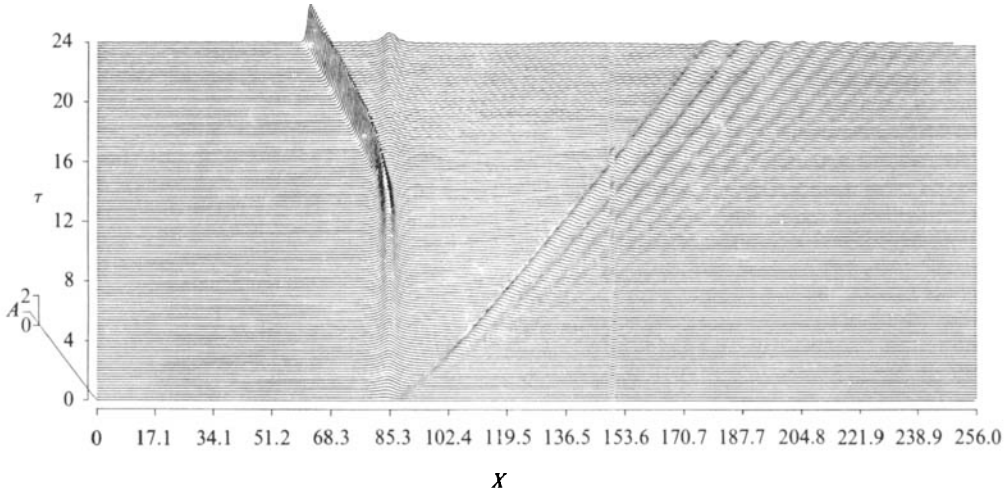

FIGURE 7. The numerical solution for the forcing function (4.4a) with $\Delta = 3$, $G_0 = 1$ and $\xi = 0.3$.

comparison is possible as she did not report any numerical results for either a or A_+. Lee (1985) numerically integrated (4.2a, b) when G' (see (4.3)) is given by $\sin^2 X'$ for $0 < X' < \pi$, and is zero elsewhere; in our notation he set $G_0 = 0.1$ and $\xi = 1.09$ (he also reported one case with $G_0 = 0.2$). In order to make some comparison with our results, we shall use the hydraulic approximation, for which we find that $\Delta_+ = 1.1$ and $\Delta_- = -0.55$. Lee describes results for (in our notation) $\Delta = -0.58$, -0.29, 0 and 0.29. The first of these falls within our transition category (ii) (§5.2), and the remainder belong to our resonant category (i). In general, his numerical results conform with the description given here. For the last three values of Δ our analytical approximations for the solitary-wave amplitude (4.38) and the downstream depression (4.16) are $a = 0.24$, 0.37 and 0.54 and $A_+ = -0.23$, -0.18 and -0.13 respectively. These compare with $a = 0.20$, 0.35 and 0.55 and $A_+ = -0.24$, -0.18 and -0.12 respectively; the agreement is good.

5.2. *Case* (*ii*): $\Delta'_- < \Delta < \Delta_-$

This case describes a transition from the resonant case $\Delta_- < \Delta < \Delta_+$ to the subcritical non-resonant case (iii) (see §5.3). In the limit $\tau \to \infty$ the solution becomes locally stationary in the forcing region, where, as in case (i), it is given by A_s, with A_s tending to A_- upstream and to A_+ downstream ($A_+ < 0 < A_-$). However, in contrast with case (i), the upstream mean level A_- is matched to a modulated cnoidal wavetrain, given by the approximate expressions (4.44$a-c$). Also, again in contrast with case (i), the downstream mean level A_+ is adjoined directly to a stationary cnoidal wavetrain, given by (4.8$a-e$) with $v = 0$, $d = A_+$ and modulus $m = m_s$. This in turn is terminated with a modulated cnoidal wavetrain of the form (4.40a–c), where now the modulus m varies over the range $0 < m < m_s$. In the hydraulic approximation $\xi \to 0$ our analytic approximation obtained in §4 implies that $\Delta_- \approx -\frac{1}{2}(12G_0)^{\frac{1}{2}}$ and $\Delta'_- \approx -(12G_0)^{\frac{1}{2}}$, while $A_\pm$ are given by (4.16). However, these approximate expressions for $A_\pm$ become increasingly inaccurate as $\Delta \to \Delta'_-$ owing to the failure of the hydraulic approximation to recognize the presence of the downstream stationary cnoidal wavetrain. For the same reason, the approximation for Δ'_- is not as good as that for Δ_-. Instead, it is possible to piece together the component parts of the solution using

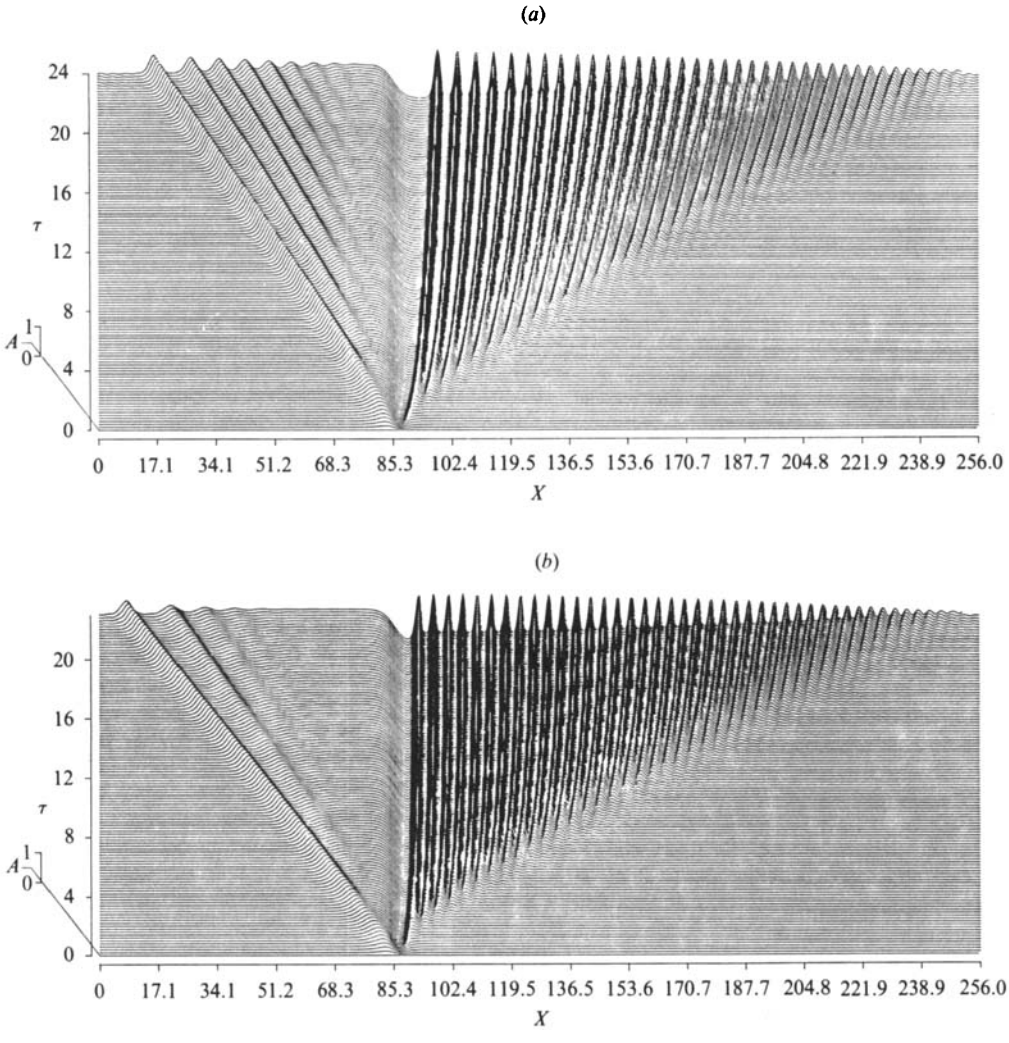

FIGURE 8. The numerical solution for the forcing function (4.4*a*) with $G_0 = 1$ and $\xi = 0.3$: (*a*) $\Delta = -1.7$; (*b*) $\Delta = -2.5$.

the modulated cnoidal wavetrains of §4.4, the stationary cnoidal wavetrain and the stationary solution in the forcing region. This approach has been developed by one of us (Smyth 1986), but will not be presented here as it results in some very complicated expressions involving elliptic functions. In the opposite limit $\xi \to \infty$, $\Delta_- \approx -\frac{3}{2}(G_0 K \xi^{-1})^{\frac{2}{3}}$ and $\Delta'_- \approx -3(G_0 K \xi^{-1})^{\frac{2}{3}}$, while $A_\pm$ are given by (4.30*a*). Again, however, these approximate expressions for $A_\pm$ become increasingly inaccurate as $\Delta \to \Delta'_-$, while the approximation for Δ'_- is not as good as that for Δ_-.

Some typical numerical solutions are shown in figure 8 for the forcing function (4.4*a*) with $G_0 = 1$, $\xi = 0.3$ and two values of Δ. The case $\Delta = -1.7$ corresponds to $\Delta \approx \Delta_-$. The replacement of the upstream solitary wavetrain by a modulated cnoidal wavetrain is clearly evident. However, the downstream solution consists entirely of the negative mean level A_- matched to a modulated cnoidal wavetrain, although we note that, in contrast with the fully resonant case shown in figure 4, the leading wave in the wavetrain is almost stationary. This agrees with the results obtained in §4.4

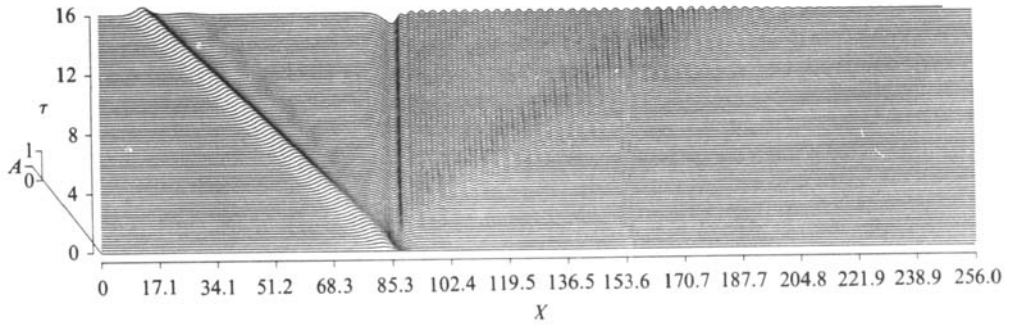

FIGURE 9. The numerical solution for the forcing function (4.4a) with $\Delta = -4$, $G_0 = 1$ and $\xi = 0.3$.

when $\Delta \to \Delta_-$ from above (see e.g. (4.42a, b)). The case $\Delta = -2.5$ represents a value of Δ in the middle of the range. All the features described above are evident. In particular, in contrast with the case $\Delta = -1.7$, we note that the upstream modulated cnoidal wavetrain is weaker, while the downstream stationary cnoidal wavetrain is well established.

5.3. *Case (iii)*: $\Delta < \Delta'_-$

This is the subcritical non-resonant case. A typical numerical solution is shown in figure 9 for the forcing function (4.4a), with $\Delta = -4$, $G_0 = 1$ and $\xi = 0.3$. The most pronounced features are the locally stationary depression in the forcing region, the generation of a finite number of upstream solitary waves to compensate for the mass contained in the depression, and the downstream stationary cnoidal wavetrain. As $\Delta \to -\infty$ with G_0 fixed, the solution reduces to the classical lee-wave configuration (see e.g. McIntyre 1972; or Patoine & Warn 1982). The hydraulic approximation predicts the depression in the forcing region (see (4.19)) and a compensating upstream triangular wave of elevation; this, of course, is resolved by the presence of dispersion into a finite number of solitary waves. The hydraulic approximation fails to predict the presence of the downstream lee waves. However, these are the central feature of an amplitude expansion in powers of G_0 (Patoine & Warn 1982), which also shows that the stationary depression tends to an upstream mean level A_- (> 0), which is matched to an upstream modulated cnoidal wavetrain, just as in case (ii). Also the downstream stationary lee waves have a mean level A_+ (< 0) and are matched to a modulated cnoidal wavetrain. However, the mean levels $A_\pm$ are $O(G_0^2 \Delta^{-3})$ and are insignificant compared with the scale of the stationary depression and the upstream solitary waves; they are not detectable in figure 9. We note here that much of the discussion in the literature on upstream influence has centred on the mean level A_- and its adjoining wavetrain, whereas it is clear from figure 9 that the predominant upstream disturbances are the solitary waves which are formed to compensate for the mass contained in the stationary depression over the forcing region.

5.4. *Case (iv)*: $\Delta > \Delta_+$

This is the supercritical non-resonant case. A typical numerical solution is shown in figure 10 for the forcing function (4.4a) with $\Delta = 4$, $G_0 = 1$ and $\xi = 0.3$. The most pronounced features are the locally stationary elevation over the forcing region, and a downstream modulated cnoidal wavetrain. The hydraulic approximation predicts

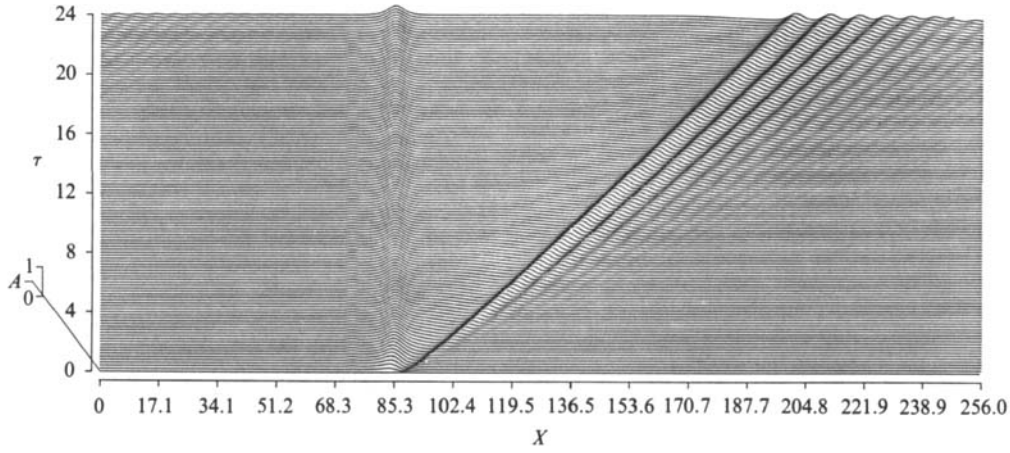

FIGURE 10. The numerical solution for the forcing function (4.4*a*) with $\Delta = 4$, $G_0 = 1$ and $\xi = 0.3$.

the elevation in the forcing region (see (4.19)) and a compensating downstream triangular depression wave; this, of course, is resolved by dispersion into an oscillatory wavetrain.

6. Discussion; numerical solutions for negative forcing

Here we shall discuss the numerical solutions of (4.2*a*, *b*) obtained with the forcing functions (4.4*a*, *b*) with $G_0 < 0$. From our numerical results we have identified three regimes.

6.1. *Case* (*i*): $\Delta_-^* < \Delta < \Delta_+^*$

This is the resonant case; $\Delta_\pm^*$ are functions of G_0 and ξ and satisfy the inequality $\Delta_-^* < 0 < \Delta_+^*$. Some typical numerical solutions are shown in figure 11 for the forcing function (4.4*a*) with $\Delta = 0$, $G_0 = -1$ and $\xi = 0.3$ in figure 11 (*a*), or $\xi = 2.0$ in 11 (*b*). In both cases, solitary waves are sent upstream, and a rather confused oscillatory wavetrain is sent downstream. However, the two cases, representing respectively weak and strong dispersion, differ considerably in detail, particularly over the forcing region.

Let us first consider the case of weak dispersion, shown in figure 11 (*a*). Here it is appropriate to use the hydraulic approximation of §4.1 as a guide to interpreting our numerical results. In the hydraulic approximation the equations to be solved are (4.9*a*, *b*) or, in characteristic form, (4.10*a*–*c*), and the solution is given by (4.11). For $\Delta^2 < -12G_0$ there exists a critical value of X_0', $X_{0\mathrm{d}}'$, where $-12G(X_{0\mathrm{d}}') = \Delta^2$; here we recall that X_0' is the initial position of the characteristic. All characteristics emanating from the $-X_{0\mathrm{d}}' < X_0' < X_{0\mathrm{d}}'$ possess turning points, while all the remaining characteristics have no turning points. Thus shocks form over the forcing region, and, unlike the case of positive forcing, the effects of dispersion are significant in the forcing region as well as in the formation of waves upstream and downstream. Further, the solution does not settle down into a stationary state in the forcing region. For instance, with $\Delta = 0$, in the hydraulic approximation a single stationary shock forms at $X' = 0$ with positive (negative) elevation in $X' > 0$ (< 0). However, from figure 11 (*a*) we see that the effect of dispersion on the region in $X > 0$ with positive elevation is to cause the

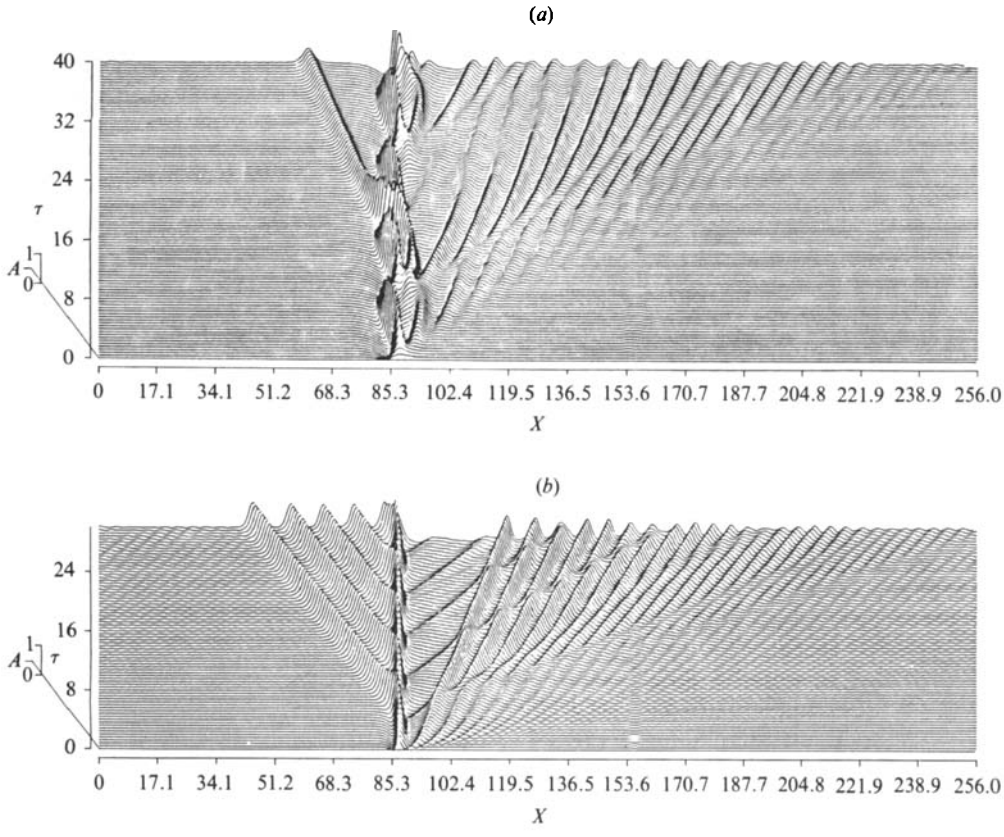

FIGURE 11. The numerical solution for the forcing function (4.4a) with $\Delta = 0$, $G_0 = -1$: (a) $\xi = 0.3$; (b) $\xi = 2.0$.

formation of a solitary-type wave which propagates upstream. If this solitary-type disturbance has insufficient mass then it decays to zero when it is free of the forcing region; examples of this process can be seen in figure 11(a). However, if the disturbance obtains sufficient mass then a solitary wave will form and propagate upstream; one such wave can be seen in figure 11(a). As each solitary-type disturbance forms and propagates upstream, simultaneously an oscillatory wavetrain is sent downstream. Finally, based on this analysis, we conjecture that as $\xi \to 0$, $\Delta_{\pm}^{*} \approx \pm(-12G_0)^{\frac{1}{2}}$, although, owing to the fact that dispersion is always significant, these boundaries are not well defined. Malanotte-Rizzoli (1984) has described some numerical solutions of a forced KdV equation, which fall into this category. In our terminology, the forcing function was $G_0 \operatorname{sech}^4 \xi X$ with $G_0 = -1$ and $\xi = 0.14$. Although her results were obtained with a non-zero initial condition, they are similar to those obtained by us.

Next we consider the case of strong dispersion shown in figure 11(b). The solution now reaches a quasistationary state in the forcing region. Disturbances with positive mass form at regular intervals and produce solitary waves which propagate upstream, and form a solitary wavetrain; this upstream behaviour is similar to the upstream behaviour for positive forcing described in §5.1. As each solitary wave forms, a corresponding wave is sent downstream. These waves travel faster than the modulated cnoidal wavetrain which terminates the downstream depression, and hence interact with it.

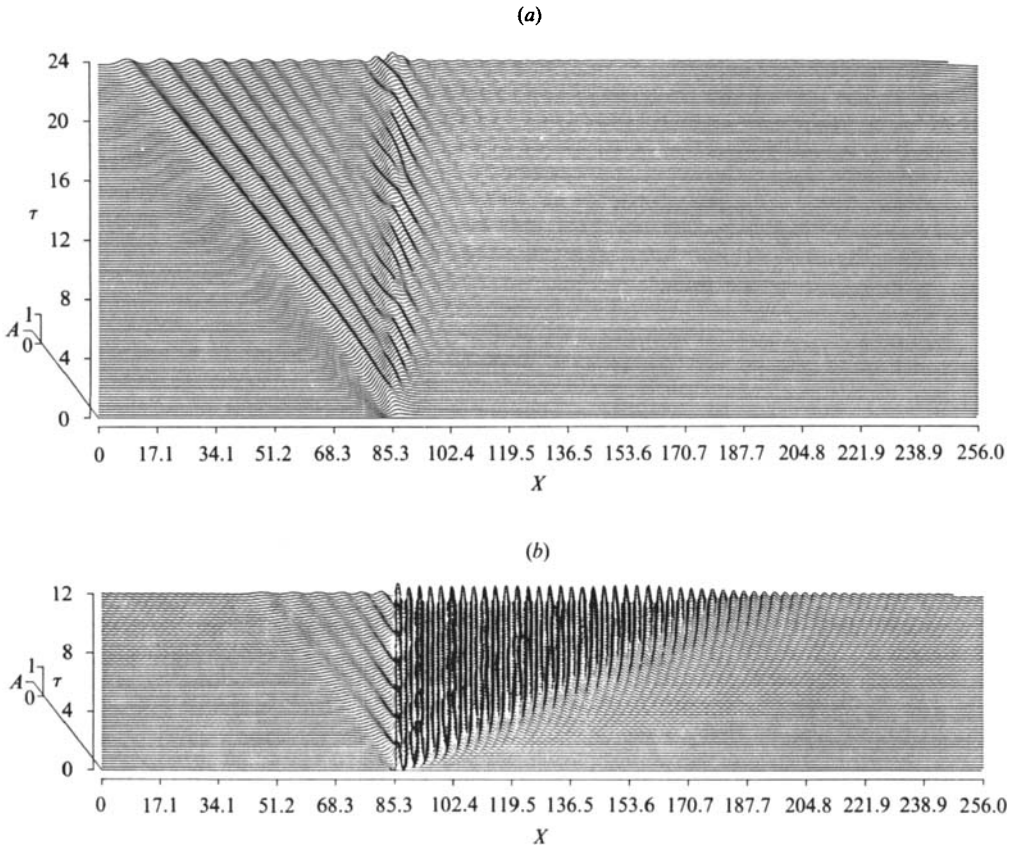

FIGURE 12. The numerical solution for the forcing function (4.4*a*) with $\Delta = -4$, $G_0 = -1$: (*a*) $\xi = 0.3$; (*b*) $\xi = 2.0$.

6.2. *Case (ii)*: $\Delta < \Delta^*_-$

This is the subcritical non-resonant case. Some typical numerical solutions are shown in figure 12 for the forcing function (4.4*a*) with $\Delta = -4$, $G_0 = -1$ and $\xi = 0.3$ in figure 12(*a*), or $\xi = 2.0$ in figure 12(*b*), corresponding to weak and strong dispersion respectively. Let us first consider the case of weak dispersion. In the hydraulic approximation of §4.1, a localized stationary solution with positive mass is formed over the forcing region and is given by (4.19). This is compensated for by an upstream triangular wave of depression, which is given by an expression similar to (4.20*a*, *b*); this, of course, is resolved by dispersion into an oscillatory wavetrain. However, examination of figure 12(*a*) shows that due to the effects of dispersion the solution in the forcing region is not stationary, although it is primarily a disturbance with positive mass. There is also evidence in figure 12(*a*) of rather weak lee waves being formed downstream. As $|\Delta|$ increases, or $|G_0|$ decreases, the lee waves become more pronounced.

The case of strong dispersion is shown in figure 12(*b*). The formation of a non-stationary disturbance with positive mass in the forcing region and a compensating upstream oscillatory wavetrain are again evident. However, the downstream lee-wave train is now the dominant feature. Patoine & Warn (1982) described some numerical solutions of (4.2*a*, *b*). In our terminology, the forcing function was (4.4*b*) with $G_0 = -1$, $\Delta = -2.45$ and $\xi = 0.78$. Their results are similar to those shown in figure 12(*b*).

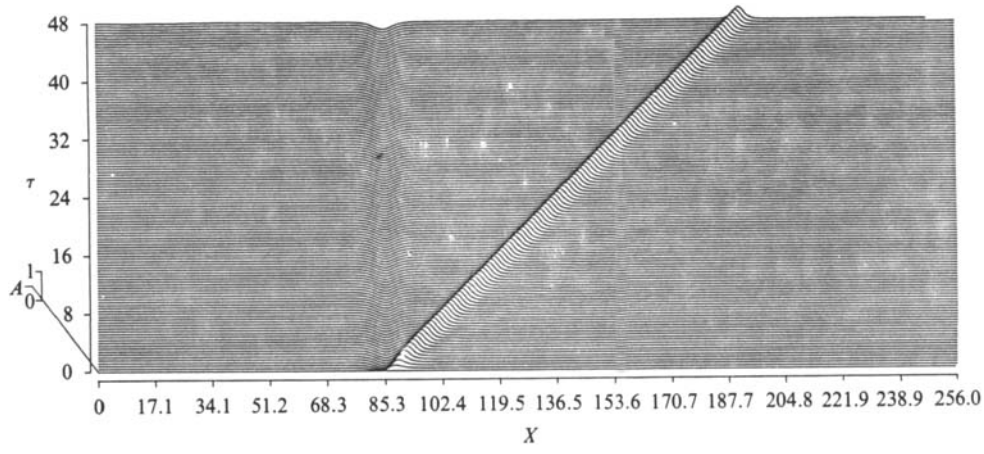

FIGURE 13. The numerical solution for the forcing function (4.4a) with $\Delta = 3$, $G_0 = -1$ and $\xi = 0.3$.

6.3. *Case (iii)*: $\Delta > \Delta_+^*$

This is the supercritical non-resonant case. A typical numerical solution is shown in figure 13 for the forcing function (4.4a) with $\Delta = 3$, $G_0 = -1$ and $\xi = 0.3$. A stationary depression is formed in the forcing region, and a compensating solitary wave is being swept downstream. In this case, these results can be predicted from the hydraulic approximation of §4.1, in which the stationary solution in the forcing region is given by (4.19) with a compensating downstream triangular wave of elevation; this, of course, is resolved by dispersion into a finite number of solitary waves.

7. Conclusions

In totality, our numerical results show that the forced KdV equation (4.2a) provides a useful model to describe the flow of a stratified fluid over topography for both the resonant and non-resonant cases, and for both subcritical and supercritical flow. Further, our supporting analysis in §4 demonstrates the utility of the hydraulic approximation in predicting the general nature of the flow field, particularly in the forcing region over the topography. One of the interesting features of our results is the appearance in many cases of significant upstream disturbances. These are either solitary waves when the localized forcing over the topography produces a positive disturbance upstream, or an oscillatory wavetrain when the disturbance has negative polarity. Here we recall that positive (negative) polarity occurs when the solitary waves of the free KdV equation have the same (opposite) polarity to the topographic forcing. It is noteworthy that these upstream disturbances are not the rather weak long wave motions calculated by Benjamin (1970), Keady (1971) or McIntyre (1972). Instead they are undoubtedly related to the strong upstream disturbances observed by Baines (1977, 1979, 1984). Downstream disturbances can also be categorized as either solitary waves or oscillatory wavetrains according to the polarity of the downstream disturbance produced by the localized forcing. For non-resonant subcritical flow there will also be a stationary lee-wave field formed. The lee waves are the one feature that cannot be predicted from the hydraulic approximation. However, we note that even when lee waves are formed they do not necessarily constitute the dominant feature of the total flow field. Furthermore, in many cases,

the downstream disturbance contains no lee waves, and is not stationary. This suggests that caution should be used in interpreting data from experiments and observations as evidence of lee waves. It is useful in this context to consider how relevant the resonant cases are likely to be *vis-à-vis* the non-resonant cases. Our numerical results show that the resonant band is defined by $\Delta_- < \Delta < \Delta_+$ (and also $\Delta'_- < \Delta < \Delta_-$ to some extent) for positive forcing, and $\Delta^*_- < \Delta < \Delta^*_+$ for negative forcing. Our estimates for $\Delta_\pm$ and $\Delta^*_\pm$ show that these scale with $G_0^{\frac{2}{3}}$ for $\xi \to 0$, or $(G_0 \xi^{-1})^{\frac{2}{3}}$ for $\xi \to \infty$. In general, the width of the resonant band increases with the magnitude of the topographic forcing, suggesting that in many applications the resonant theory presented here may be more appropriate than the traditional linearized theories. If, for simplicity, we restrict attention to the hydraulic limit, then we expect the resonant theory to hold when $\Delta < (12|G_0|)^{\frac{1}{2}}$. Evaluating this criterion in terms of the scaling (4.1) and the definition of Δ (3.1*c*) we find that it becomes

$$\left|\frac{V}{c_n} - 1\right| < |\mu|^{\frac{1}{2}} \max |\alpha G_n|^{\frac{1}{2}}, \tag{7.1}$$

where G_n is related to the bottom topography $\alpha g(X)$ by (2.15*b*) and the coefficient μ is defined by (3.6*b*). It is pertinent to note here that, *inter alia*, the width of the resonant band is proportional to $|\mu|^{\frac{1}{2}}$, and, by virtue of the scaling (4.1), the magnitude of the solution is proportional to $|\mu|$. Hence we expect resonance to be important whenever $|\mu|$ is not too small. This is certainly the case for waves on the free surface of a homogeneous fluid (see (7.6) below), and for stratified fluids in which $N^2(z)$ (see (2.1)) varies significantly over the fluid depth. An extreme instance of this is the two-layer fluid for which $N^2(z)$ is a δ-function; in this case μ is given by (7.3*a*) and is non-zero except under very special circumstances. On the other hand μ is $O(\beta)$ if $N^2(z)$ is constant over the fluid depth, and is small for a Boussinesq fluid, for which $\beta \to 0$. In this case it would be necessary to include a cubic term in the forced KdV equation (3.6*a*) (see Gear & Grimshaw (1983) or Miles (1979) for a discussion of this for the free KdV equation).

There have been numerous experiments and observations of the flow of a stratified fluid over topography. Of particular relevance to the theory presented here are the experiments by Baines (1977, 1979, 1984) and the observations by Farmer & Smith (1980) and Farmer & Denton (1985) of tidally generated flow over a sill. Farmer & Smith and Farmer & Denton record the results of a number of observations for different parameter settings, and, although the field situation is complicated by the time-dependence of the basic flow, their observations are generally consistent with the theoretical results obtained here. Particularly pertinent is the fact that they found internal hydraulic theory useful in categorizing their observations, and in describing the flow field directly over the topography. Baines (1977, 1979) describes experiments of stratified flow over topography, with $N^2(z)$ nearly constant. Although he observed significant upstream disturbances that were first-order in the obstacle height and propagated with the long-wave speed, we are unable to compare his observations directly with our theory, since the coefficient μ was very small for the experimental situation. As we commented above, this necessitates the inclusion of a cubic term in the forced KdV equation (3.6*a*). However, Baines (1984) has given a comprehensive account of the flow of a two-layer fluid over topography based on a series of experiments and internal hydraulic theory. Most of his discussion relates to the flow field over the topography and the upstream disturbance, and, with due allowance for the effects of friction, his results are generally consistent with our theory. For a

two-layer fluid of total depth h, lower-layer depth d and densities ρ_1 and ρ_2 in the upper and lower layers respectively, we find that the modal function is

$$\phi(z) = \begin{cases} \dfrac{z}{d} & \text{for } 0 < z < d, \\ \dfrac{h-z}{h-d} & \text{for } d < z < h, \end{cases} \tag{7.2a}$$

$$c^2 = \frac{(\rho_2+\rho_1)\,d(h-d)}{2(\rho_1 d+\rho_2(h-d))}. \tag{7.2b}$$

This result is obtained from (2.10a–c), where we put $\rho_{0z} = (\rho_1-\rho_2)\,\delta(z-d)$ and, for simplicity, assume that the upper boundary is rigid; the Boussinesq parameter $\beta = 2(\rho_2-\rho_1)/(\rho_2+\rho_1)$. Next, evaluating μ and λ from (3.6b, c), we find that

$$\mu = \frac{3c^2}{(\rho_2+\rho_1)}\left\{\frac{\rho_2}{d^2}-\frac{\rho_1}{(h-d)^2}\right\}, \quad \lambda = \frac{c^2}{3(\rho_2+\rho_1)}\{\rho_2 d+\rho_1(h-d)\}. \tag{7.3a, b}$$

For the experiments described by Baines (1984) the topography had a long lengthscale, and so the criterion for the validity of our resonant theory is (7.1). Evaluating μ from (7.3a) and G_n from (2.15b), this becomes

$$\left(\frac{V}{c}-1\right)^2 < \left|R\frac{\alpha g_0}{h}\right|, \tag{7.4a}$$

where

$$R = \frac{3}{2}\frac{\rho_1 h d^2(h-d)}{\{\rho_1 d+\rho_2(h-d)\}^2}\left\{\frac{\rho_1}{(h-d)^2}-\frac{\rho_2}{d^2}\right\}. \tag{7.4b}$$

Here g_0 is the maximum height of the topography, which, in view of the experimental configuration, we have placed in the upper boundary. In our terminology, the experiments were all for positive forcing, and most satisfied the criterion (7.4a). Hence they mostly correspond to our case (i), in which the main upstream effect is the solitary wavetrain (see figure 4). Indeed, in many of his experiments Baines (1984) observed an upstream undular bore, which, apart from frictional effects, corresponds to our solitary wavetrain. Further, he found good quantitative agreement between the upstream elevation and the predictions of internal hydraulic theory. In the weakly nonlinear limit internal hydraulic theory will give the same expression for this upstream elevation as that found by us in §4.1 (see (4.16)). Hence his experiments provide an indirect confirmation of the theory described here.

Finally, we note that, although our main concern has been with stratified fluids, our results can be applied to the generation of gravity waves on the free surface of a homogeneous fluid. Indeed, for a homogeneous fluid

$$\phi(z) = \frac{z}{h} \quad \text{for } 0 < z < h, \tag{7.5a}$$

$$c^2 = h. \tag{7.5b}$$

Here we put the Boussinesq parameter $\beta = 1$. Evaluating μ and λ from (3.6b, c), we find that

$$\mu = \frac{3}{2h}, \quad \lambda = \tfrac{1}{6}h^2. \tag{7.6}$$

The counterpart to (7.3*a*) for the validity of the resonant theory is

$$\left(\frac{V}{c}-1\right)^2 < \left|\frac{3}{2}\frac{\alpha g_0}{h}\right|. \tag{7.7}$$

Recently Huang *et al.* (1982), in a towing tank experiment, observed the generation of upstream solitary waves for flows near criticality. In our terminology, the experiments were for positive forcing, and satisfied the criterion (7.7). Hence they correspond to our case (i), and the observations show a marked similarity with our figure 4. Wu & Wu (1982) investigated numerically some Boussinesq long-wave equations, and modelled the towed obstacle with a travelling pressure distribution. They obtained results generally consistent with ours, and with the experimental results of Huang *et al.* (1982). More recently, Lee (1985) has derived a forced KdV equation analogous to (4.2*a*, *b*) to describe flow over bottom topography, and has compared numerical solutions of this equation with his experimental results. With due allowance for the effects of friction, the agreement is very good, the only exception being phase differences in the downstream lee-wave field. We have discussed his numerical solutions in §5, and recall that they are consistent with ours.

One of us (N.S.) acknowledges support from the Australian Research Grants Scheme under Grant 83/15835.

Appendix. Extension of the analysis for deep fluids

The derivation of the amplitude equation (3.6*a*) requires the implicit assumption that the channel depth h is $O(1)$ with respect to the small parameter ϵ (i.e. the dimensional depth scales with h_1). In this section we replace this with the hypothesis that the channel depth scales with ϵ^{-1}, and we put $h = H\epsilon^{-1}$, where H is $O(1)$ with respect to ϵ. At the same time we shall assume that in the deep fluid region, where z scales with ϵ^{-1}, the density stratification is weak, and specifically the Brunt–Väisälä frequency $N(z) \to \epsilon(N_0)$ as $z \to \infty$. It then follows from (2.1) that

$$\rho_0 = \tilde{\rho}_0(z)\exp(-\epsilon^2 N_0^2 z), \tag{A 1a}$$

where

$$\tilde{\rho}_0(z) \to \rho_\infty \quad \text{as } z \to \infty. \tag{A 1b}$$

In the deep fluid region the vertical variable z is replaced by Z, where

$$Z = \epsilon z. \tag{A 2}$$

We also replace q, u with Q, U, where

$$q = \epsilon Q(X, T, Z), \quad u = \epsilon U(X, T, Z). \tag{A 3}$$

Then, to leading order in ϵ, in the deep fluid region the governing equations (2.2*a–d*) become

$$U_X + \frac{\mathrm{D}}{\mathrm{D}T}\zeta_Z = 0, \tag{A 4a}$$

$$\rho_0(Z)\frac{\mathrm{D}U}{\mathrm{D}T} + Q_X = 0, \tag{A 4b}$$

$$\rho_0(Z)\frac{\mathrm{D}^2\zeta}{\mathrm{D}T^2} + Q + \rho_0(Z)N_0^2\zeta = 0, \tag{A 4c}$$

where

$$\rho_0(Z) = \rho_\infty \exp(-\epsilon N_0^2 Z). \tag{A 4d}$$

Here we recall that $\mathrm{D}/\mathrm{D}T$ is defined by (2.8e) and the error terms are relatively $O(\epsilon)$. Eliminating U, Q and omitting terms that are relatively $O(\epsilon)$, we find that

$$\frac{\mathrm{D}^2}{\mathrm{D}T^2}(\zeta_{XX}+\zeta_{ZZ})+N_0^2\zeta_{ZZ}=0. \tag{A 5}$$

The boundary conditions (2.6a, b) reduce to, again omitting $O(\epsilon)$ error terms,

$$\zeta=0 \quad \text{at } Z=H. \tag{A 6}$$

Because of the large horizontal and vertical lengthscales in the deep fluid region, the upper boundary is effectively rigid, to leading order in ϵ. The solution of (A 5) and (A 6) is readily obtained from Fourier transforms in X and T. This solution is then matched with the corresponding solution in the lower fluid region, where z is $O(1)$.

Consider first the non-resonant case. In the lower fluid region we again use the expansion (2.7), where ζ_0, q_0 and u_0 satisfy (2.8a–d) and the bottom boundary condition (2.9a). The other boundary condition (2.9b) is now replaced by an appropriate matching condition. In the deep fluid region we put

$$\zeta=\alpha\zeta_0(X,T,Z)+\ldots, \tag{A 7a}$$

$$Q=\alpha Q_0(X,T,Z)+\ldots, \tag{A 7b}$$

$$U=\alpha U_0(X,T,Z)+\ldots, \tag{A 7c}$$

where ζ_0 satisfies (A 5) and (A 6), and Q_0, U_0 are then found from (A 4a–c). Matching with (2.7) shows that

$$q_0, u_0 \to 0 \quad \text{as } z\to\infty, \tag{A 8a}$$

$$\zeta_0(X,T;z\to\infty)=\zeta_0(X,T,Z\to 0). \tag{A 8b}$$

Equation (A 8a) replaces the boundary condition (2.9b), and (A 8b) provides a lower boundary condition for (A 5). In the lower fluid region the solution is again obtained from the normal-mode expansion (2.12a–c) where (A 8a) now requires that in the eigenvalue problem (2.10a–c) for $\phi_s(z)$ the boundary condition (2.10c) is replaced by

$$\phi_{sz}\to 0 \quad \text{as } z\to\infty. \tag{A 9}$$

The orthogonality condition is again satisfied. The remaining development in §2 is unchanged and (2.14a–c) hold as before, with the solution (2.16a) or (2.17). In this non-resonant case the deep fluid region is passive, to leading order in ϵ. Once $A_s(X,T)$ has been found, $\zeta_0(X,T;z\to\infty)$ is calculated from (2.12a), and the solution in the deep fluid region is obtained by solving (A 5) with the boundary conditions (A 6) and (A 8a).

In the resonant case we again use the expansion (3.1a) in the lower fluid region, where now the mode $\phi_n(z)$ satisfies the boundary condition (A 9). In the deep fluid region we put

$$\left.\begin{aligned}\zeta&=\alpha^{\frac{1}{2}}\zeta_0(X,Z;\tau)+\alpha\zeta_1+\ldots,\\ Q&=\alpha^{\frac{1}{2}}Q_0(X,Z;\tau)+\alpha Q_1+\ldots,\\ U&=\alpha^{\frac{1}{2}}U_0(X,Z;\tau)+\alpha U_1+\ldots,\end{aligned}\right\} \tag{A 10}$$

where ζ_0 satisfies (A 5) and (A 6), and U_0, Q_0 are then found from (A 4a–c). Since now $\mathrm{D}/\mathrm{D}T\approx c_n\,\partial/\partial X$, we find that (A 5) reduces to

$$c_n^2(\zeta_{0XX}+\zeta_{0ZZ})+N_0^2\zeta_0=0, \tag{A 11a}$$

$$Q_0=\rho_0(Z)\,c_n^2\,\zeta_{0Z}, \quad U_0=-c_n\,\zeta_{0Z}. \tag{A 11b}$$

The balance between nonlinearity and dispersion now requires that $\epsilon = \alpha^{\frac{1}{2}}$. Matching with (3.1$a$) shows that

$$\zeta_0(X, Z \to 0; \tau) = A(X, \tau)\,\phi_n(z \to \infty), \tag{A 12a}$$

$$q_1 \to \rho_\infty c_n^2\,\zeta_{0Z}(X, Z = 0; \tau) \quad \text{as } z \to \infty, \tag{A 12b}$$

$$u_1 \to -c_n\,\zeta_{0Z}(X, Z = 0; \tau) \quad \text{as } z \to \infty. \tag{A 12c}$$

Equation (A 12a) provides a lower boundary condition for (A 11a), while the upper boundary condition is (A 6). The solution is

$$\zeta_0 = \phi_n(\infty)\frac{1}{2\pi}\int_{-\infty}^{\infty} \frac{\sinh R(H-Z)}{\sinh RH} \exp(\mathrm{i}kX)\,\mathscr{F}(A)\,\mathrm{d}k, \tag{A 13a}$$

where

$$\mathscr{F}(A) = \int_{-\infty}^{\infty} A(X, \tau) \exp(-\mathrm{i}kX)\,\mathrm{d}X, \tag{A 13b}$$

$$R = \left(k^2 - \frac{N_0^2}{c_n^2}\right)^{\frac{1}{2}}. \tag{A 13c}$$

Here R is defined so that if R is real then $R > 0$, while if R is pure imaginary, $(\mathrm{Im}\,R)\,k > 0$. As $H \to \infty$ the terms involving H in (A 13a) are replaced by $\exp(-RZ)$, where the definition of R ensures that the solution is either exponentially decaying or is an outgoing wave.

In the lower fluid region ζ_1, q_1 and u_1 again satisfy (3.2a–d) with the omission of the term A_{XX} in (3.2c). However, the upper boundary condition (3.2e) is now replaced by (A 12b); (A 12c) is then automatically satisfied (see e.g. (3.2b)). The solution is again given by (3.3a), where A_{s1} again satisfies (3.4a). However, now the term A_{XXX} in M_{sX} (see (3.4b)) is omitted and replaced by $q_{1X}\,\phi_s(z)$ as $z \to \infty$. Here q_1 is obtained from (A 12b) and (A 13a). Proceeding as in §3, we find that the amplitude equation that replaces (3.6a) is

$$-\frac{1}{c_n}(A_\tau + \Delta A_X) + \mu A A_X + \hat{\lambda}\mathscr{B}(A_X) + \tfrac{1}{2}G_n(X) = 0, \tag{A 14a}$$

where

$$\mathscr{B}(A) = \frac{1}{2\pi}\int_{-\infty}^{\infty} R \coth RH \exp(\mathrm{i}kX)\,\mathscr{F}(A)\,\mathrm{d}k, \tag{A 14b}$$

$$2I_n\hat{\lambda} = \rho_\infty c_n^2\,\phi_n^2(\infty). \tag{A 14c}$$

Finally, matching with the inner expansion proceeds as described in §3; in particular, the initial condition is again (3.7a).

Equation (A 14a) can be recognized as a forced evolution equation of KdV type. In the limits $H \to \infty$ and $N_0 \to 0$ it reduces to a forced version of the equation derived by Benjamin (1967) and Davis & Acrivos (1967) to describe internal solitary waves in deep fluids. Using the same scaling as employed in §4, with the dispersive coefficient λ replaced by $\hat{\lambda}$, we find that (A 14a) and (3.7a) become

$$-A^*_{\tau^*} - \Delta^* A^*_X + 6A^* A^*_X + \mathscr{B}(A^*_{X^*}) + G^*_X(X) = 0, \tag{A 15a}$$

$$A^*(X, 0) = 0. \tag{A 15b}$$

With the exception of the dispersive term, (A 15a, b) are identical to (4.2a, b). In particular, the conclusions derived from the hydraulic approximation in §4.1 may be applied here as well. Further, we expect the effects of dispersion in (A 15a) to be

similar to its role in (4.2a), which we have discussed in §4. Thus, although we have not obtained numerical solutions of (A 15a, b), we anticipate that the solutions will possess the same qualitative features obtained for (4.2a, b), and described in §§5 and 6.

REFERENCES

AKYLAS, T. R. 1984 On the excitation of long nonlinear water waves by a moving pressure distribution. *J. Fluid Mech.* **141**, 455–466.

BAINES, P. G. 1977 Upstream influence and Long's model in stratified flows. *J. Fluid Mech.* **82**, 147–159.

BAINES, P. G. 1979 Observation of stratified flow over two-dimensional obstacles in fluid of finite depth. *Tellus* **31**, 351–371.

BAINES, P. G. 1984 A unified description of two-layer flow over topography. *J. Fluid Mech.* **146**, 127–167.

BENJAMIN, T. B. 1967 Internal waves of permanent form in fluids of great depth. *J. Fluid Mech.* **29**, 559–592.

BENJAMIN, T. B. 1970 Upstream influence. *J. Fluid Mech.* **40**, 49–79.

COLE, S. L. 1985 Transient waves produced by flow past a bump. *Wave Motion* **7**, 579–587.

DAVIS, R. E. & ACRIVOS, A. 1967 Solitary internal waves in deep water. *J. Fluid Mech.* **29**, 593–607.

FARMER, D. M. & DENTON, R. A. 1985 Hydraulic control of flow over the sill in Observatory Inlet. *J. Geophys. Res.* **90**, 9051–9068.

FARMER, D. M. & SMITH, J. D. 1980 Tidal interaction of stratified flow with a sill in Knight Inlet. *Deep-Sea Res.* **27A**, 239–254.

FORNBERG, B. & WHITHAM, G. B. 1978 A numerical and theoretical study of certain nonlinear wave phenomena. *Phil. Trans. R. Soc. Lond.* A **289**, 373–404.

GEAR, J. & GRIMSHAW, R. 1983 A second order theory for solitary waves in shallow fluids. *Phys. Fluids* **26**, 14–29.

GRIMSHAW, R. 1983 Solitary waves in density stratified fluids. In *Nonlinear Deformation Waves* (ed. V. Nigul & J. Engelbrecht), pp. 431–447. Springer.

GUREVICH, A. V. & PITAEVSKII, L. P. 1974 Nonstationary structure of a collisionless shock wave. *Sov. Phys. JETP* **38**, 291–297.

HAMMACK, J. L. & SEGUR, H. 1978 Modelling criteria for long water waves. *J. Fluid Mech.* **84**, 359–373.

HUANG, D.-B., SIBUL, G. J., WEBSTER, W. C., WEHAUSEN, J. V., WU, D.-M. & WU, T. Y. 1982 Ships moving in the transcritical range. In *Proc. Conf. on Behaviour of Ships in Restricted Waters, Varna*, vol. 2, pp. 26-1–26-10.

KEADY, G. 1971 Upstream influence in a two-fluid system. *J. Fluid Mech.* **49**, 373–384.

LEE, S.-J. 1985 Generation of long water waves by moving disturbances. Ph.D. thesis, California Institute of Technology.

MCINTYRE, M. E. 1972 On Long's hypothesis of no upstream influence in uniformly stratified or rotating flow. *J. Fluid Mech.* **52**, 209–242.

MALANOTTE-RIZZOLI, P. 1984 Boundary-forced nonlinear planetary radiation. *J. Phys. Oceanogr.* **14**, 1032–1046.

MILES, J. W. 1978 On the evolution of a solitary wave for very weak nonlinearity. *J. Fluid Mech.* **87**, 773–783.

MILES, J. W. 1979 On internal solitary waves. *Tellus* **31**, 456–562.

PATOINE, A. & WARN, T. 1982 The interaction of long, quasi-stationary baroclinic waves with topography. *J. Atmos. Sci.* **39**, 1018–1025.

SMYTH, N. F. 1986 Modulation theory solution for resonant flow over topography. *Proc. R. Soc. Lond.* (to appear).

WARN, T. & BRASNETT, B. 1983 The amplification and capture of atmospheric solitons by topography: theory of the onset of regional blocking. *J. Atmos. Sci.* **40**, 28–38.

WHITHAM, G. B. 1965 Non-linear dispersive waves. *Proc. R. Soc. Lond.* A **283**, 238–261.

WHITHAM, G. B. 1974 *Linear and Nonlinear Waves*. Wiley.

WU, D.-M. & WU, T. Y. 1982 Three-dimensional nonlinear long waves due to moving surface pressure. In *Proc. 14th Symp. on Naval Hydrodynamics, Ann Arbor.*